ARL 65-234

DIGITAL COMPUTER STUDIES OF CONDENSATION IN EXPANDING ONE-COMPONENT FLOWS

KENNETH R. SIVIER

THE UNIVERSITY OF MICHIGAN
ANN ARBOR, MICHIGAN

NOVEMBER 1965

Contract AF 33(615)-2307
Project No. 7116
Task No. 7116-01

AEROSPACE RESEARCH LABORATORIES
OFFICE OF AEROSPACE RESEARCH
UNITED STATES AIR FORCE
WRIGHT-PATTERSON AIR FORCE BASE, OHIO

FOREWORD

This technical report was prepared by the College of Engineering, The University of Michigan, Ann Arbor, Michigan on Contracts AF 33(657)-8867 and AF 33(615)-2307 for the Aerospace Research Laboratories, Office of Aerospace Research, United States Air Force. The research reported herein was accomplished on Task 7116-01, "Internal Flow Research," of Project 7116, "Energy Conversion Research," under the technical cognizance of Mr. Everett Stephens of the Thermo-Mechanics Research Laboratory of ARL.

This report represents a continuation of the work reported by James L. Griffin in ARL 63-206 and terminates the present phase of the work being done, under the above contracts, on computer techniques for studying condensation phenomena.

ABSTRACT

This report discusses a digital computer program for calculating the vapor condensation that occurs in expanding, one-component flows. A discussion is presented of modifications made in Griffin's original program. Emphasis is placed on the reasons for the modifications and their effect on the numerical results.

The results of a parametric study (using the computer program) of condensation onset in nitrogen flows are presented and compared with experimental data. Several methods of presenting and correlating condensation onset data are used. One of these produces a remarkable correlation of the numerical results. The comparison between the experimental and numerical data shows that the computer program is able to reproduce satisfactorily the qualitative features of the condensation produced and to yield a relatively good quantitative picture of condensation onset in nitrogen.

TABLE OF CONTENTS

LIST OF ILLUSTRATIONS

LIST OF ILLUSTRATIONS (continued)

LIST OF SYMBOLS

A	nozzle cross-sectional area, in^2 or cm^2.
c_p	vapor specific heat at constant pressure, dyne - cm/gm - ^oK.
c_v	vapor specific heat at constant volume, dyne - cm/gm - ^oK.
d	diameter of axisymmetric nozzle, in. or cm.
D	constant used in the Tolman surface tension correction for drop size (see Eq. (2-4)), cm.
h	height of two-dimensional nozzle, in. or cm.
$\bar{h}$	reduced throat height for two-dimensional (wedge) nozzle (see Eq. (3-5)), cm.
ln	logarithm to the base e.
log	logarithm to the base 10.
$\dot{m}$	total mass flow through the nozzle, lbs/sec or gm/sec.
M	Mach number.
$\dot{N}_d$	number flux of foreign nuclei through the nozzle, particles/sec.
L	latent heat of vaporization, dyne - cm/gm.
p	pressure, psia.
$\hat{p}$	ratio of ambient pressure of the flow to the pressure that would have existed (at the nozzle point in question) in a corresponding isentropic expansion, i. e., $\hat{p} = p/p_i$.
$p_{\infty, c}$	vapor pressure corresponding to the temperature T_c, psia.
r	radius of axisymmetric nozzle or of condensed drop, depending on context, in. or cm.
r_d	radius of foreign nuclei, cm.

$\bar{r}$ reduced throat radius for axisymmetric (conical) nozzle (see Eq. 3-4)), cm.

Δr increase in drop radius, due to growth by condensation, during one computer step Δx, cm.

R universal gas constant = 8.314×10^7 dyne - cm/gmol - ^oK.

$\dot{S}$ total surface area flux of all drops in the flow, cm^2/sec.

$\dot{S}_d$ surface area flux of foreign nuclei (see Eq. (2-7)), cm^2/sec.

$\Delta \dot{S}_d$ increase in surface area flux, due to condensation on drops formed on foreign nuclei (see Eq. (2-9)), during one computer step Δx, cm^2/sec.

t time, seconds.

T temperature, degrees Kelvin.

$\hat{T}$ ratio of ambient temperature of the flow to the temperature that would have existed (at the nozzle point in question) in a corresponding isentropic expansion, i.e., $\hat{T} = T/T_i$.

ΔT_c supersaturation temperature decrement (see Sec. 3.4), degrees Kelvin.

$\Delta T_{i,c}$ isentropic supersaturation temperature decrement (defined by Eq. (3-3)), degrees Kelvin.

T_ℓ temperature of the drop; assumed to equal the saturated vapor temperature corresponding to ambient vapor pressure, ^oK.

U flow velocity, feet/sec or cm/sec.

x distance along nozzle axis, measured from the throat, in. or cm.

Δx computer step along the nozzle, cm.

Δx_i initial computer step size used at start of nucleation, cm.

$Z_{i,c}$ condensation onset correlation parameter defined by Eq. (3-9).

Greek Symbols

α accommodation coefficient.

γ ratio of the specific heats, c_p/c_v.

ϵ nucleation onset test parameter; used by the program to determine the point along the nozzle at which condensation calculations are to begin.

η equivalent mass fraction of foreign nuclei defined by Eq. (2-5).

θ geometrical half-angle of the nozzle, degrees.

μ gram molecular weight of the vapor.

σ surface tension, dyne/cm.

σ_∞ surface tension of an infinite, plane surface, dyne/cm.

ρ vapor density, grams/cm^3.

ρ_ℓ liquid density, grams/cm^3.

Superscript

* nozzle throat condition.

Subscripts

c condition at condensation onset.

i isentropic expansion.

o initial vapor condition.

sat condition at vapor saturation.

1. INTRODUCTION

This report is concerned with the current form of a digital computer program that was devised to permit study of condensation processes occurring in expanding vapor flows. The original program was formulated by Griffin and is described in Ref. 1. Since the completion of Griffin's work, a number of program modifications have been made. These modifications have improved the program's numerical accuracy (i. e., improved the agreement between the numerical results and experimental data) and increased the range of application, convenience of use, and running speed of the program. A detailed description of the program, from the computer programmer's point-of-view, is presented in Ref. 2. A summary of the mathematical model used for the program also is presented in Ref. 2.

The principal features of the program may be summarized as follows:

1. The general, steady, one-dimensional, diabatic flow equations are used. These equations account for the heat added to and the mass removed from the uncondensed vapor due to the condensation process. The arrangement of these equations follows in detail the discussion given by Wegener and Mack[3], except that the problem has been specialized to the case of a one-component vapor.

2. Originally the program considered only homogeneous condensation; i. e., all condensed drops were formed initially by homogeneous nucleation. The program now permits the consideration of a simple case of heterogeneous condensation; i. e., when the vapor passes its saturation point, condensation begins by growth on a single class of foreign nuclei having an arbitrary number flux and arbitrary, but uniform, radii.

Manuscript released June 1965 by the author for publication as an ARL Technical Documentary Report.

3. All condensation is assumed to take place from the vapor to the liquid phase. The homogeneous nucleation process, represented by the Becker-Döring theory as given by Frenkel[4], is critically dependent on the value of liquid surface tension. To improve the nucleation rate prediction, the variation of surface tension with drop size is approximated by the relation given by Tolman[5].

4. The vapor pressure curve is approximated by a quadratic curve fit to empirical data (in the form of 1/T vs log p) above the triple point and by a straight line below the triple point. The latter approximation is equivalent to a Clausius-Clapeyron curve fit and is useful for extrapolations of the vapor pressure curve to low temperatures.

5. The drops are assumed to grow according to the free molecular growth law given by Stever[6]. In this calculation, the drop temperature is taken to be equal to the equilibrium saturated vapor temperature corresponding to the local ambient pressure of the vapor.

6. Agglomeration of the drops is neglected.

7. The condensation calculations are carried out in a stepwise manner through a fixed, straight walled nozzle (either wedge or conical). The step size is automatically varied to keep the amount of vapor condensed (and, hence, the condensation-produced changes in the flow variables) near some suitable pre-selected value during each program step.

8. At each point where results are printed out, the stagnation pressure behind a normal shock wave is computed. This computation is based on the local values of ambient pressure and Mach number in the condensing flow, but the computation completely neglects the effects of the condensed phase being carried by the flow.

9. At each point where results are printed out, "isentropic" values of ambient pressure, ambient density, ambient temperature, normal shock stagnation pressure, and Mach number are computed. These values correspond to the flow that would have existed, at the point in question, if condensation had been absent; they are computed on the basis of local area ratio only. These values are compared with those computed for the condensing flow for a running indication of the extent of condensation caused deviations from isentropic flow.

The principal program modifications (to Griffin's original program) are discussed in Section 2 below from the points-of-view of both the reasons for the changes and their effects on program operation and results. Section 3 presents the results of a parametric study of nitrogen condensation, that was made using the program, and shows the comparison of these results with experimental data.

2. PROGRAM MODIFICATIONS

2.1 Approximation to the Vapor Pressure Curve

Griffin's program[1] incorporated a Clausius-Clapeyron relation, i. e.,

$$\ln p = B - C\left(\frac{1}{T}\right) \tag{2-1}$$

to provide vapor pressure data for the calculations. The constants B and C were evaluated by satisfying Eq. (2-1) at two empirical data points. Although this provided a convenient method for supplying vapor pressure data to the program, it often represented a poor approximation to the empirical data. As an example, vapor pressure data for nitrogen are shown in Fig. 1 plotted in the form of log p versus 1/T. These data are typical of all saturation curves in that the curve is very nearly bilinear with a significant slope discontinuity at the triple point. Obviously, a single linear fit to these data will not be a generally good representation. This is particularily true for extrapolations to very low temperatures; a common situation in view of the large supersaturation that often occurs. This situation is indicated in Fig. 1 by an extrapolation based on the straight line between the critical and triple points.

To improve this situation, the vapor pressure data are now represented by two curves fitted to the empirical data:

(1) a quadratic approximation,

$$\frac{1}{T} = A_1 + B_1 \log p + C_1 (\log p)^2 \quad , \tag{2-2}$$

is used above the triple point (the quadratic term approximates the slight non-linearity that is usually found above the triple point) and

(2) a linear approximation (essentially the Clasius-Clapeyron equation),

$$\frac{1}{T} = A_2 + B_2 \log p \quad , \tag{2-3}$$

is used below the triple point.

The latter approximation was chosen so that extrapolations to temperatures below the range of available data could be based on a relation of the Clausius-Clapeyron form.

2. 2 Surface Tension Correction and Evaluation of the Tolman Constant

The numerical results presented by Griffin[1] showed good qualitative agreement with the experimental data of Nagamatsu and Willmarth[7]. However, an arbitrary nine percent decrease (at $40^{\circ}K$) in surface tension was required to yield a reasonable quantitative agreement. For those calculations, Griffin assumed a linear variation of surface tension with temperature (essentially an Eötvös-type relation for surface tension), fitted to empirical data, and also assumed that the surface tension of a critical drop (drop nucleus) of condensate would be that of an infinite plane liquid surface. These same calculations showed that the critical drops have radii of about 1. 3 times the diameter of a nitrogen molecule. Thus, at the point of maximum nucleation rate, these critical drops are far from having infinite radii, in terms of the molecular diameter, and some significant effect on surface tension, due to drop size, must be expected[(1)].

[(1)] This approach completely ignores the argument[8, 9, 10, 11] that the classical Becker-Döring nucleation theory, and its dependency on the macroscopic properties of the liquid, may have no validity in the cases where the critical drop size is of the order of the molecular diameter. The objective here is to adjust rationally the calculations based on this theory such that the results will have some practical value. Furthermore, the program is constructed such that a major change in the nucleation theory can be introduced without major changes in the rest of the program.

To approximate the effect of drop radius, the approximation given by Tolman[5] was added to the program; i. e. ,

$$\sigma = \frac{\sigma_\infty}{1 + \frac{D}{r}} \tag{2-4}$$

where

σ_∞ = surface tension of an infinite plane surface,

r = drop radius,

and

D = a dimension closely related to the intermolecular distance in the liquid drop.

Tolman argues that D will be reasonably constant over a wide range of drop sizes because of its close relationship to the intermolecular distance in the liquid. A value for D on the order of 10^{-8} cm is suggested in Refs. 5 and 12. However, Tolman[5] points out that the theoretical computations are not sufficiently reliable to give exact values of D.

In view of the uncertainty about the value of D that should be used, Eq. (2-4) was assumed as a surface tension correction for the program and D was taken as a constant to be evaluated from experimental data. To do this for the case of molecular nitrogen, a series of computations(1) was made, at various values of D, and compared with the Nagamatsu-Willmarth data. The results of these computations, for values of D from 0 to 1. 5 x 10^{-8} cm, are shown in Figs. 2 and 3. It was concluded that a value of D of 0. 65 x 10^{-8} cm gave a nucleation

---

(1) The physical properties of nitrogen used in these calculations are summarized in Table I and are discussed in Section 3. 2 below. The other input parameters are listed in Table II.

"break" which best approximated the experimental data. (Surface tension is important only to the nucleation phase of the condensation process and therefore D can influence only the location and sharpness of the nucleation break.)

It is noted that the value of 0.65×10^{-8} cm for D is of the order predicted by Tolman. In the vicinity of the nucleation break, critical drops have minimum radii of about 4×10^{-8} cm. Thus, the Tolman correction reduces the surface tension by a maximum of about 15% from the plane surface value. It should be noted that there is no evidence that this value of D will apply to vapors other than molecular nitrogen.

2.3 Variable Step Size

In the original program[1], a constant (but arbitrary) step size was used throughout a given problem. (Here, a step represents a given increment in the distance along the nozzle.) However, the rate (per unit distance) of condensation does not remain constant throughout the expansion. Initially, nucleation is very slow. These initial nuclei represent only a negligible amount of condensate but are important because of the condensation-through-growth that occurs on them. As the expansion carries the state of the vapor deep into the region of nucleation, the condensation rate rises abruptly to some maximum value. The energy released by this condensation heats the remaining vapor and causes the vapor state to move out of the region of nucleation and toward the vapor saturation curve (see Fig. 2). The growth process now becomes dominant and the condensation rate decreases continuously as the vapor state approaches saturation. As a typical example, Fig. 4 shows the computed condensation rate history for the Nagamatsu-Willmarth expansion. In view of this history of condensation rate, it has been found that a step size that is sufficiently small to avoid significant errors in the stepwise approximation to the condensation process when the rate

is high, may result in an unnecessarily slowly running program where drop growth is dominant. In addition, the selection of a step size, appropriate to the maximum condensation rate for any given problem, requires prior knowledge of what that value of condensation rate is.

To relieve this situation, the program now has provisions for automatically changing the step size as the condensation rate varies. Essentially, the program tests the amount of condensate formed during a given step. If this amount exceeds some preselected maximum value, the step size is halved; if it is less than a preselected minimum value, the step size is doubled. Selection of appropriate limits for the amount condensed per step results in as fine an approximation as desired. Typically, condensation of about 0.1 percent of the total mass flow (obtained, for example, by minimum and maximum limits of 0.05 and 0.15 percent per step) has been found acceptable.

The condensation rate is extremely low during the initial phases of nucleation. However, significant errors can result by taking large steps during this portion of the process (see Sec. 3.3 below). To handle this situation, the program contains a control which prohibits changing the step size until some minimum amount of condensate has accumulated. This permits the necessary detail in the calculation during the initial nucleation phase, while allowing necessary step size adjustments when condensation rates become high and when growth is dominant.

2.4 Heterogeneous Condensation

The computer program is concerned mainly with homogeneous condensation. However, heterogeneous condensation (i.e., condensation on particles, or foreign nuclei, in the flow) can produce major changes in the condensation history. Wegener[13] briefly compares the processes of homogeneous heterogeneous condensation. In the latter case, the vapor begins to condense on the foreign nuclei as soon as the expansion crosses the vapor pressure curve and the vapor becomes

supersaturated. If enough nuclei are present, the resulting condensation effects may prevent the vapor from reaching a state where homogeneous nucleation can occur. In the limit, the condensation can be rapid enough to force the expansion to follow the vapor pressure curve. The results of an experimental study of these effects are presented in Ref. 14.

To approximate the heterogeneous condensation process, Griffin's program was modified to accommodate foreign nuclei. Provisions were made to introduce into the problem a single family of particles having a radius of r_d and a flow rate of N_d particles per second. Growth of these particles is computed in exactly the same manner as for nuclei formed by homogeneous nucleation. In particular, the gas dynamic interactions between the particles and the flow are totally neglected. These particles are given as initial data and begin to grow as soon as the vapor becomes supersaturated. However, the program continues to search for homogeneous nucleation and, in general, the calculation includes both heterogeneous and homogeneous condensation.

The results of several heterogeneous nitrogen condensation calculations[1] are shown in Fig. 5; a "clean" (homogeneous condensation only) expansion is included for comparison. For these examples, the selection of r_d and $\dot{N}_d$ was made on an "equivalent" mass flow basis; i. e.,

$$\eta \dot{m} \equiv \dot{N}_d \rho_\ell \left(\frac{4}{3} \pi r_d^3\right) \tag{2-5}$$

= equivalent mass flow represented by the flux of foreign nuclei

---

[1] The physical properties of nitrogen used in these calculations are summarized in Table I and are discussed in Sec. 3. 2 below. The other input parameters are listed in Table II.

where

η = equivalent mass fraction of the vapor flow occurring as foreign nuclei.

The nuclei number flux then becomes

$$\dot{N}_d = \frac{3\dot{m}}{4\pi \rho_\ell} \frac{\eta}{r_d^3} \tag{2-6}$$

In selecting values of η for the calculations, the results of Ref. 14 were used as a guide. Those results suggested that $\eta = 1 \times 10^{-4}$ would produce a negligible effect on the condensation process, while $\eta = 1 \times 10^{-2}$ would produce a major effect.

The results presented in Fig. 5 show that, although the equivalent mass flux of foreign nuclei is an important parameter, the size and total area flux of the particles are more important to the heterogeneous condensation process. The rate of mass condensation through growth, during any program step, is directly proportional to the total flux of surface area, $\dot{S}$, of all the drops present. Initially, in the case of the foreign nuclei (all having the same size),

$$\dot{S}_d = 4\pi r_d^2 \dot{N}_d \tag{2-7}$$

The relation between $\dot{N}_d$ and r_d is given by Eq. (2-6) and Eq. (2-7) can be written

$$\dot{S}_d = \frac{3\dot{m}}{\rho_\ell} \frac{\eta}{r_d} \tag{2-8}$$

Thus, for a given value of η, the initial heterogeneous condensation rate will vary inversely with particle size. Furthermore, the growth of initially small drops will result in a more rapid increase in surface area and a corresponding increase in

condensation rate. This is illustrated by noting that, during any given step, the change in area flux due to condensation on drops formed on foreign nuclei is given by

$$\Delta \dot{S}_d = \frac{6\dot{m}\eta}{\rho_\ell \, r_d^2} r \, \Delta r = 2\dot{S}_d \left(\frac{r}{r_d}\right) \Delta r \qquad (2\text{-}9)$$

The results presented in Fig. 5 illustrate these effects. For the two cases with equal values of $\dot{S}_d$ and, therefore, equal initial condensation rates, only the one with the smaller particles (and, incidentally, a smaller value of η) exhibits a growth history such that homogeneous nucleation does not occur. This is directly due to the rapid change in surface area as the smaller particles grow. The three constant η cases are illustrative of the effect of initial particle size on the flow process. The smallest particles result in almost a saturated expansion; the largest in almost an "all homogeneous condensation" expansion.

3. CONDENSATION IN EXPANDING NITROGEN FLOWS

3.1 Introduction and Condensation Onset Criterion

Primarily as an example of the utility of the condensation computer program, a parametric study of condensation in expanding nitrogen flows has been made. The study had as its objective the evaluation of the effects of initial pressure and temperature and of geometry (geometric expansion rate) on the supersaturation that occurs. To provide a uniform standard for condensation onset for comparison of the results from the various calculations, it was assumed that a significant (and experimentally detectable) amount of condensation had occurred when the ambient pressure of the flow had risen one (1) percent above the corresponding isentropic pressure that would have existed in the flow in the absence of condensation. That is, at the point of condensation onset

$$\hat{p}_c = \frac{p_c}{p_{i,\,c}} = 1.01 \tag{3-1}$$

3.2 Physical Properties of Nitrogen

The values of the several physical properties of nitrogen, used in this study, are summarized in Table I. The linear approximations for surface tension, latent heat of vaporization (liquid/vapor phase change), and density as functions of temperature, were obtained as "eyeball" straight line fits to data given in Ref. 15. The quadratic and linear vapor saturation curve approximations were obtained from manually calculated least squares curve fits to the data given in Ref. 16.

The value of the specific heat at constant pressure, c_p, was calculated from the relation

$$c_p = \frac{R}{\mu}\left(\frac{\gamma}{\gamma - 1}\right) \tag{3-2}$$

where it was assumed that $\gamma = 1.4$. This relationship between c_p and γ was

necessary so that the velocities computed from the two equations,

$$U = \sqrt{2c_p (T_o - T)}$$

and

$$U = M\sqrt{\gamma \frac{R}{\mu} T} \quad ,$$

would be in agreement. Use of values of c_p corresponding to the low vapor temperatures that can occur in condensing expansions, would have required the use of a variable value for γ. This refinement was considered to be an unnecessary complication at this stage of program development.

The accommodation coefficient, α, was taken as 1.0 in the absence of information suggesting a more appropriate value. This selection has little influence on most of the results reported below since α plays a role only during the growth process and nucleation is the major process involved in reaching $\hat{p} = 1.01$.

The constant D, used in the Tolman drop size surface tension correction, was given the value of 0.65×10^{-8} cm, determined from the Nagamatsu-Willmarth data as described in Section 2.2 above.

3.3 Selection of Δx_i and ϵ

Early in the study, it became evident that the results were being influenced by Δx_i, the initial step size, and by ϵ, the sensitivity parameter used to determine the onset of significant nucleation (see Ref. 1, pgs. 11 through 15). A number of runs were made to indicate the form and extent of these effects. The results are presented in Fig. 6 for nitrogen at supply conditions of 100 psia and 298^{o}K, and with conical geometries having expansion half-angles of 5 and 30 degrees. These

results were obtained with Δx held constant at its initial value. It is apparent that Δx_i produces the major effect. The choice of ϵ produces large effects only when Δx_i is too large. When Δx_i is sufficiently small (on the order of one percent of $\bar{r}$), the choice of ϵ is essentially unimportant.

Although the choice of Δx_i can change significantly the initial phases of the computed condensation history, the effect decreases rapidly as condensation continues. This is illustrated in Fig. 7. For the case shown, the effect of Δx_i becomes negligible by the time the pressure has risen to about 10 percent above the isentropic value. Also shown in Fig. 7 are examples of the effect of changing the step size after an initial part of the condensation has been computed with step size Δx_i. These results indicate that no significant changes in the results occur due to increasing step size if the initial phase of the process has been computed using a suitably small Δx_i.

The computations, leading to the results shown in Figs. 6 and 7, indicated that 175 to 200 steps of Δx_i were required to achieve $\hat{p} = 1.01$ when Δx_i was suitably small and $\epsilon = 1 \times 10^{-8}$. This was taken as the criterion for selecting Δx_i for all the studies reported below. Checks of the validity of this criterion at supply pressures of 1000 and 5000 psia showed that it was, if anything, conservative. It is therefore concluded that the results reported below have not been influenced by the choice of Δx_i.

3.4 Results of the Parametric Calculations

The parametric condensation study consisted of several series of calculations that investigated the influence of initial vapor conditions and flow geometry. These calculations were organized as follows:

1. Variations of geometry with initial pressure and temperature fixed.
2. Variation of initial pressure with geometry and initial temperature fixed.

3. Variation of initial temperature with geometry and initial pressure fixed.
4. Variation of both initial pressure and temperature such that the initial vapor state remained on the same isentrope. Geometry was fixed.

The input data for these calculations are listed in Table II and the results are summarized in Table III. The results are also compared with the nitrogen vapor pressure curve in Fig. 8.

The several series of calculations are discussed in more detail in Sections 3. 4. 1 through 3. 4. 4 below and condensation onset data, in terms of the isentropic supersaturation temperature decrement $\Delta T_{i,\ c}$, are presented in Figs. 9 through 12. This temperature decrement is defined as

$$\Delta T_{i,\ c} \equiv T_{sat} - T_{i,\ c} \quad . \tag{3-3}$$

Note that this decrement is measured along the isentrope established by the initial vapor conditions. This isentropic decrement differs slightly from the actual temperature decrement,

$$\Delta T_c \equiv T_{sat} - T_c$$

since

$$\hat{T} = \frac{T}{T_i} = 1.01 \text{ to } 1.02 \quad \text{for} \quad \hat{p} = 1.01$$

However, the data are presented in terms of $\Delta T_{i,\ c}$ because this form is more easily applied to the general problem of estimating the supersaturation in nozzle flows.

3. 4. 1 Variation of Geometry

The unit area gradients for straight walled, inviscid nozzle flows can be written as

$$\left(\frac{1}{A}\frac{dA}{dx}\right)_{conical} = \frac{2}{\bar{r}\sqrt{A/A^*}} \tag{3-4}$$

and

$$\left(\frac{1}{A}\frac{dA}{dx}\right)_{wedge} = \frac{2}{\bar{h}(A/A^*)} \tag{3-5}$$

where

$$\bar{r} = r^*/\tan\theta$$

and

$$\bar{h} = h^*/\tan\theta$$

Thus, these unit area gradients are functions of the geometry of the nozzle only through the reduced throat radius, $\bar{r}$, for conical nozzles or the reduced throat height, $\bar{h}$, for wedge nozzles.

The calculations reported here were made for conical nozzles only. The geometries used in the calculations were as follows:

$\bar{r}$, cm	r*, cm	d*, inches	θ, degrees
1.46	0.127	0.10	5.00
.72	0.127	0.10	10.00
.47	0.127	0.10	15.00
.35	0.127	0.10	20.00
.22	0.127	0.10	30.00
.72	0.0635	0.05	5.06
.72	0.254	0.20	19.42
1.44	0.254	0.20	10.00
3.60	0.635	0.50	10.00

These selections provide over one order of magnitude variation in $\bar{r}$ as well as several checks with nozzles having very different throat diameters and expansion angles but equal values of $\bar{r}$.

Calculations of condensation onset for the above geometries were made for initial pressures of 100, 1000, and 5000 psia. All calculations were for an initial temperature of 298°K. The results, in terms of $\Delta T_{i,\,c}$, are presented in Fig. 9. These results demonstrate that $\bar{r}$ is the correct parameter for describing the effect of geometry on supersaturation. As expected, an increase in expansion rate (through decreasing $\bar{r}$) results in greater supersaturation. This occurs because, along a given isentrope, the nucleation rate can be considered as a function of the ambient vapor temperature only. (In the vicinity of condensation onset, the nucleation rate is increasingly extremely rapid with decreasing temperature.) It has been found that, for a given initial vapor state, the amount of condensate required to produce onset ($\hat{p} = 1.01$) is essentially independent of expansion rate. Increasing values of geometric expansion rate are associated with decreasing residency times for each temperature along the isentrope and, therefore, correspondingly decreasing amounts of condensate are formed at each temperature. As a result, the expansion must continue to lower temperatures (for higher expansion rates) before sufficient condensation has occurred to produce the onset effect.

3. 4. 2 Variation of Initial Pressure

The effect of initial pressure on condensation onset was investigated by making calculations for initial pressures from 5 to 7500 psia. All calculations were made for an initial temperature of 298°K and an $\bar{r}$ of 0. 72 ($d^* = 0.10$ inches and $\theta = 10$ degrees).

The results of the calculations, presented in Fig. 10, show a general increase in the supersaturation temperature decrement with decreasing pressure, for the range of pressures considered. This trend must ultimately reverse itself at lower pressures; e. g., in cases where the vapor becomes saturated at a temperatures below, say, 25°K, $\Delta T_{i,\,c}$ cannot exceed the saturation temperature even if the condensation reaction becomes "frozen".

Figure 10 also indicates that the supersaturation will decrease to zero as the saturation point approaches the critical point. This result is interesting in that no feature of the program or of the various input data identifies the critical point as being in any way unique[1]. The pressure range over which $\Delta T_{i,\ c}$ decreases rapidly toward zero is the range in which condensation onset points occur at temperatures above the triple point temperature. Therefore, this is a region of certain vapor-to-liquid phase change and one in which there is no uncertainty in the vapor pressure data used to compute the onset point. (Vapor pressure data for temperatures near the onset temperature are obtained by extrapolation for cases with initial pressures below about 900 psia.) In addition, the calculations show that the critical drops are very large in this region; their diameters increase from 14 $\mathring{A}$ for the 2000 psia case to 34 $\mathring{A}$ for 7500 psia. This suggests some validity in the classical nucleation theory since macroscopic physical properties may apply to such large nuclei. These arguments lend support to the validity of the rapid decrease in supersaturation, at the higher pressures, shown in Fig. 10.

The "flat" in the data shown in Fig. 10 is associated with initial pressures where two conditions prevail: (1) the saturation points occur above the triple point and (2) the onset points occur at temperatures below the triple point. A discontinuous change in the slope of the vapor pressure curve occurs at the triple point; the slope is higher below the triple point. This results in a more rapidly increasing nucleation rate (with decreasing temperature) and an earlier condensation onset. This effect apparently balances the tendency of $\Delta T_{i,\ c}$ to increase with decreasing pressure and results in the constant value of $\Delta T_{i,\ c}$ over this range of pressures.

---

(1) The program does not consider the real gas effects occurring at the higher initial pressures and in the vicinity of the critical point.

3. 4. 3 Variation of Initial Temperature

A very short series of calculations was made to investigate the effect of initial temperature. These calculations were made at initial temperatures of 298, 450, 700, and 1100°K with an initial pressure of 1000 psia and an $\bar{r}$ of 0. 72 ($d^* = 0.10$ inches and $\theta = 10$ degrees). The maximum temperature, 1100°K, was selected to place that point on the isentrope defined by the 10 psia, 298°K case. The results are shown in Fig. 11. The increase of $\Delta T_{i,c}$ with increasing T_o is analogous to the increase in $\Delta T_{i,c}$ with decreasing p_o (Fig. 10); both effects are associated with decreases in the initial density of the vapor.

3. 4. 4 Constant Initial Entropy

The effect on the supersaturation temperature decrement of varying initial conditions, while holding the entropy constant, is shown in Fig. 12. The following results were obtained for the isentrope determined by the initial conditions of 100 psia and 298°K:

T_o, °K	M_{sat}	$T_{i,c}$, °K	$M_{i,c}$	$\Delta T_{i,c}$, °K	$\left(\frac{1}{A}\frac{dA}{dt}\right)_c$, 10^4 sec^{-1}
55. 5	. 18	33. 6	1. 81	21. 6	4. 91
60. 0	. 66	33. 5	1. 99	21. 7	5. 03
100. 0	2. 02	33. 8	3. 13	21. 4	4. 70
298. 0	4. 69	34. 6	6. 17	20. 5	2. 66
1000. 0	9. 26	35. 8	11. 61	19. 4	1. 19
2000. 0	13. 28	36. 5	16. 41	18. 7	0. 74

(T_{sat} = 55. 16°K for all cases)

Since for each expansion the state of the vapor at saturation is the same, the effect shown in Fig. 12 is thought to be that of geometric expansion rate alone. The last column in the table above shows that the unit time rate of change of area decreases with increasing supply temperature (due to an increasing $M_{i,c}$ and, hence, increasing A/A^* at condensation onset) and therefore the decrease in $\Delta T_{i,c}$ with increasing T_o shown in Fig. 12 is analogous to the decrease due to increasing $\bar{r}$ shown in Fig. 9.

In running the two lowest temperatures in this series, no computer problems developed as a result of having subsonic saturation Mach numbers. In the minimum temperature case, the Mach number at which the ϵ (= 1.0×10^{-8}) test was satisfied was about 1.2 so that no computations were required in the neighborhood of M = 1. Figure 12 shows that $\Delta T_{i,c}$ reaches a maximum of about 21.7°K at the saturation temperature; this gives 1.80 as the minimum onset Mach number for this isentrope. Although no problem was experienced here, computer difficulties would occur for initial temperatures near the saturation value at higher pressure levels.

3.5 Correlation of Condensation Onset Results

With the extensive condensation onset data available from the parametric study, it appeared desirable to search for some form of systematic correlation of the results. As shown in Secs. 3.4.1 and 3.4.4 above, a definite relation exists between the supersaturation temperature decrement, $\Delta T_{i,c}$, and the geometric expansion rate. One would expect, however, that the rate of change of some state variable would be more representative of the expansion kinetics that lead to supersaturation. In the case of density[1], the time rate of change can be written as

$$\frac{1}{\rho}\frac{d\rho}{dt} = \frac{1}{\rho}\frac{d\rho}{dM}\frac{dM}{dA}\frac{dA}{dx}\frac{dx}{dt} \qquad (3\text{-}6)$$

Assuming a one-dimensional, isentropic flow and using the area gradients given by Eqs. (3-4) and (3-5), the reduced time rate of change of density becomes

---

(1) Pressure or temperature could have been chosen here. However, density has the advantage that the final form for $(1/\rho)\, d\rho/dt$ does not depend explicitly on the ratio of the specific heats, γ. On the other hand, for example, the pressure and density rates are related by the expression

$$\frac{1}{p}\frac{dp}{dt} = \gamma\left(\frac{1}{\rho}\frac{d\rho}{dt}\right)$$

$$\left(\frac{1}{\rho}\frac{d\rho}{dt}\right)_{conical} = -\frac{2UM^2}{(M^2 - 1)\,\bar{r}\,\sqrt{A/A^*}} \tag{3-7}$$

or

$$\left(\frac{1}{\rho}\frac{d\rho}{dt}\right)_{wedge} = -\frac{2UM^2}{(M^2 - 1)\,\bar{h}\,(A/A^*)} \tag{3-8}$$

The results (in terms of $\Delta T_{i,c}$) of the parametric study have been compared on the basis of the unit rate of change of density in Fig. 13. As an aid to applying the results to the prediction of condensation onset, $(1/\rho)\, d\rho/dt$ has been evaluated in terms of the isentropic flow variables at the onset point, i. e., $M_{i,c}$ and $U_{i,c}$. The area ratio A/A^* is a function only of the point along the nozzle at which $\hat{p} = 1.01$.

It is obvious that this presentation of the onset results does not provide a general correlation. However, an inspection of Fig. 13 provides two interesting hints:

1. The $\bar{r}$ - variation curve for $p_o = 100$ psia and the constant entropy (but varying p_o and T_o) curve are essentially coincident. The common factor between these two curves is that their initial conditions lie on a common isentrope.

2. A factor of roughly 10 in $-(1/\rho)\, d\rho/dt$ exists between the 100 psia and 1000 psia $\bar{r}$ - variation curves for equal values of $\Delta T_{i,c}$.

These observations lead to the consideration of the parameter

$$Z_{i,c} \equiv -\left(\frac{1}{\rho}\frac{d\rho}{dt}\right)_{i,c} \Big/ \frac{p_o}{T_o^{3.5}} \tag{3-9}$$

as one appropriate for correlating the condensation data. The factor $p_o/T_o^{3.5}$ was selected because (1) it is constant along an isentrope (for $\gamma = 1.4$)and (2) it contains the effect of p_o suggested by observation (2) above.

The result of correlating all of the computed condensation onset data on the basis of the above parameter, is shown in Fig. 14. A significant collapse of the data has occurred. With the exception of the very high pressure conditions (saturation temperatures above about 90^oK), all of the data fall within a $\Delta T_{i,c}$ band varying in width from $\pm 1^oK$ for values of $Z_{i,c}$ around 10^{10} to about $\pm 0.5^oK$ for $Z_{i,c}$ greater than 10^{12}.

The reason for the success of the correlation is not known, but its utility is evident. As an example an isentrope is included in Fig. 14 for the following conditions:

$$p_o = 5000 \text{ psia}$$
$$T_o = 1000^oK$$
$$d^* = 0.050 \text{ inches}$$
$$\theta = 15 \text{ degrees}$$

The intersection of this isentrope with the condensation onset band predicts a supersaturation temperature decrement of 21.4 ± 0.7^oK.

3.6 Comparison with Experimental Data

Figure 15 shows a comparison of the results of the parametric condensation calculations with condensation onset data from several different hypersonic nozzles. The data by Vas and Koppenwallner and the data by Griffith, et al., are presented as given in Refs. 17 and 18, respectively. The Daum data were taken from Figs. 2 and 3 of Ref. 19 and are presented using (1) the supply temperature at condensation onset as given and (2) the supply temperature at which $\hat{p} = 1.01$. The application

of this onset criterion is seen to improve the agreement between Daum's data and the numerical results. The Nagamatsu and Willmarth points were obtained also by applying the $\hat{p}_c = 1.01$ criterion to the data presented in Ref. 7. Finally, the onset curve from Ref. 19 is also shown.

The agreement between the experimental data and the numerical results, as presented in Fig. 15, is reasonably good. Because of the serious questions about the validity of the computations at low condensation temperatures (e. g., the ability of the nucleation theory to represent the vapor/solid state change, the small size of the nuclei, the extrapolated vapor pressure curve), this favorable comparison anywhere below the Nagamatsu-Willmarth points must be considered fortuitous. The trend of the experimental data at the lowest temperatures (all of which are for very high Mach numbers) suggests an effective "freezing" of the condensation "reaction" which has not been indicated by the calculations reported here. (Some unreported early test calculations, along lower isentropes, showed a sufficiently slow "reaction" to suggest that the computer would also show a trend to "frozen" condensation as the onset temperature decreases.)

The onset curve from Ref. 19 clearly does not agree with the numerical results. The suggestion is very strong that this onset curve, up to the point at which it approaches the Daum data, primarily reflects the effect of heterogeneous condensation.

The experimental data are presented in Fig. 16 as $\Delta T_{i,c}$ versus the correlation parameter $Z_{i,c}$. The comparison with the numerical results are now far less encouraging. The high Mach number data are uniformly in poor agreement with the numerical results. It appears that, on this basis, the numerical results represent, at best, a conservative estimate for $\Delta T_{i,c}$.

Calculations, of the supply temperature, T_{o_c}, at which $\hat{p} = 1.01$ at the nozzle exit, were made for two of Daum's[19] cases. The input parameters are listed in Table II. Daum's experiments were conducted in air. An estimate of the difference between air condensation and nitrogen condensation was made for the M = 15 nozzle case by making calculations using (1) the full pressure of 700 psia and (2) the partial pressure of nitrogen in 700 psia air. The computer results are:

M = 10 Nozzle	$T_{o_c} = 541^{o}K = 975^{o}R$
M = 15 Nozzle (700 psia)	$T_{o_c} = 883^{o}K = 1590^{o}R$
M = 15 Nozzle (574 psia)	$T_{o_c} = 860^{o}K = 1550^{o}R$

The values of $\Delta T_{i,c}$ corresponding to these calculated onset supply temperatures are shown in Fig. 16. As expected, these points fall within the parametric study band. More detail on the rise of the static pressure, at the M = 15 nozzle exit, with decrease in supply temperature is presented in Fig. 17. These results show the similarity in the initial pressure rise curve between the experimental and computer results. The partial pressure case gives the better agreement. This actually may approximate the physical process better, since a test run with oxygen (at its partial pressure) showed that its greater surface tension and lower partial pressure resulted in greater supersaturation than for nitrogen. This suggests that for the case of homogeneous condensation in air, the process will be started by nucleation in the nitrogen component.

Figure 17 shows also that after the initial pressure rise, the numerical results show a pressure rise that exceeds the experimental one. It is felt that this is directly due to a poor growth law and for this reason, the computer has not been used to predict quantitative results beyond nucleation.

Additional detail on the comparison between numerical and experimental results is shown in Fig. 18. In this figure, the computer results are compared with

the data from Nagamatsu and Willmarth[7], Runs 9-5 and 23-1. The $\hat{p}$ data were calculated on the basis of data given in Figs. 13, 14, and 16 of Ref. 7 and are subject to relatively large errors for $\hat{p}$ near 1.0. Unlike the Daum case, the initial $\hat{p}$ rise histories are not similar. Furthermore, when viewed in this detail, the selection of $D = 0.65 \times 10^{-8}$ cm on the basis of Figs. 2 and 3 is seen to be incorrect. A value between 0.9 and 1.3×10^{-8} cm is required to provide agreement at $\hat{p} = 1.01$. Such a selection would lead to uniformly smaller calculated values of $\Delta T_{i,c}$ but would not change the overall picture of the numerical results.

A last method of presenting (and correlating) condensation onset data has been suggested by Vas and Koppenwallner[17]. They point out that it should be approximately true that $\log (p_c/p_{\infty,c})$ is a linear function of $T_c^{-3/2}$. The results of the parametric study and the experimental data discussed above are collected in this fashion in Fig. 19. The correlation appears remarkably good. The linearity is excellent except for conditions having saturation points near the critical point. However, to illustrate that this is not a very sensitive correlation, two isentropes have been included on Fig. 19. It is clear that the correlation curve and the isentropes are very nearly parallel at their intersection. Thus, condensation onset can occur over a rather large range of temperatures along the isentrope while appearing to fall, very satisfactorily, on the correlation curve.

4. RESULTS AND CONCLUSIONS

The digital computer program discussed above has been found to be a convenient vehicle for making numerical studies of the condensation processes occurring in expanding, one-component flows. Within the limitations of the nucleation and growth theories, upon which the program is based, the program is able to describe, satisfactorily, the qualitative features of condensing, one-component flows. By adjusting one program constant so that the numerical results agree with one set of experimental data, the program was found to give a relatively good quantitative description of condensation onset in molecular nitrogen for a wide range of initial pressures and temperatures and flow geometries.

The following results and conclusions have resulted from the computer studies:

1. The determination of condensation onset requires very careful calculations during the initial phases of nucleation. The practical application of this result requires the use of very small steps along the nozzle at the beginning of the nucleation calculation. Later increases in step size have only small effects on the results. Also, it appears that the initial step size can be large if only the later portions of the condensation history are of interest.

2. The growth law appears to yield condensation rates which are initially large compared to the corresponding experimental rates. A better growth law will be required to permit reliable calculations of the entire condensation process.

3. The program has qualitatively described the heterogeneous condensation process. The effects, on the condensation history, of size and number flux of the foreign nuclei have been shown.

4. A parameter has been found that provides an excellent correlation of all the computed condensation onset results for nitrogen, except for those expansions which have saturation points approaching the critical point.

5. The computer results indicate that vapor supersaturation approaches zero as the saturation point approaches the critical point. This result occurred without providing information, identifying the critical point, in the program or in the input data.

5. REFERENCES

1. Griffin, J. L., "Digital Computer Analysis of Condensation in Highly Expanded Flows," (Univ. of Mich.) USAF Aerospace Research Labs, OAR, Report ARL 63-206, November 1963.

2. Harding, L. J., "A Digital Computer Program for Condensation in Expanding One-Component Flows," (Univ. of Mich.) USAF Aerospace Research Labs, OAR, ARL 65-58, March 1965.

3. Wegener, P. P. and Mack, L. M., "Condensation in Supersonic and Hypersonic Wind Tunnels," Advances in Applied Mechanics, Vol. V, Academic Press, 1958, pp. 307-447.

4. Frenkel, J., Kinetic Theory of Liquids, Clarendon Press, Oxford, 1956, pp. 366-400. (Also published by Dover Publications, Inc., New York).

5. Tolman, R. C., "The Effect of Droplet Size on Surface Tension," J. Chem. Phys., Vol. 17, No. 3, pp. 333-337, March 1949.

6. Stever, H. G., "Condensation in High Speed Flows," High Speed Aerodynamics and Jet Propulsion, Vol. III, pp. 526-573, Princeton University Press, Princeton, N. J., 1958.

7. Nagamatsu, H. T. and Willmarth, W. W., "Condensation of Nitrogen in a Hypersonic Nozzle," GALCIT Hypersonic Wind Tunnel Memorandum No. 6, January 1952.

8. Courtney, W. G., "Homogeneous Nucleation from Simple and Complex Systems," AIAA Preprint No. 63-494, presented at the AIAA Heterogeneous Combustion Conference, December 11-13, 1963.

9. Wegener, P. P. and Pouring, A. A., "Experiments on Condensation of Water Vapor by Homogeneous Nucleation in Nozzles," Physics of Fluids, Vol. 7, No. 33, pp. 352-361, March 1964.

10. Lothe, J. and Pound, G. M., "Reconsiderations of Nucleation Theory," J. Chem. Phys., Vol. 36, No. 8, pp. 2080-2085, April 15, 1962.

11. Courtney, W. G., "Re-examination of Nucleation and Condensation of Water," Technical Report, Thiokol Chemical Corporation, Reaction Motors Division, Denville, New Jersey, July 1964.

REFERENCES (continued)

12. Tolman, R. C., "The Superficial Density of Matter at a Liquid-Vapor Boundary," J. Chem. Phys., Vol. 17, No. 2, pp. 118-127, February 1949.

13. Wegener, P. P., "Condensation Phenomena in Nozzles," AIAA Preprint No. 63-509, presented at the Heterogeneous Combustion Conference, Palm Beach, Florida, December 11-13, 1963.

14. Arthur, P. D., "Effects of Impurities on the Supersaturation of Nitrogen In a Hypersonic Wind Tunnel," Ph. D. Thesis, Cal. Inst. of Tech., 1952.

15. Handbook of Chemistry and Physics, 41st Edition, Chemical Rubber Publishing Co., Cleveland, Ohio, 1959.

16. Tables of Thermal Properties of Gases, NBS Circular 564, U. S. Government Printing Office, Washington, D. C., 1955.

17. Vas, I. E. and Koppenwallner, G., "The Princeton University High Pressure Hypersonic Nitrogen Tunnel N-3," (Princeton U. Gas Dynamics Lab. Report 690), United States Air Force, Office of Scientific Research Report AFOSR 64-1422, July 1964.

18. Griffith, B. J., Deskins, H. E., and Little, H. R., "Condensation in Hotshot Tunnels," Arnold Engineering Development Center Report AEDC-TDR-64-35, February 1964.

19. Daum, F. L., "The Condensation of Air in a Hypersonic Wind Tunnel," IAS Paper No. 63-53, presented at the IAS 31st Annual Meeting, January 21-23, 1963. (Also published in the AIAA Journal, Vol. 1, No. 5, pp. 1043-1046, May 1963).

TABLE I

PHYSICAL PROPERTIES OF NITROGEN

Physical Property	Value	Source
α	1.0	———
γ	1.4	———
c_p	1.036×10^7, $\frac{\text{dyne-cm}}{\text{gm-}^\circ\text{K}}$	Eq. (3-2)
μ	28.02, gm.	Ref. 15
σ	$23.94 - 0.1933\ T_\ell$, dyne/cm.	Straight line fit to data from Ref. 15
ρ_ℓ	$1.181 - 4.8 \times 10^{-3}\ T_\ell$, gm/cm^3	Straight line fit to data from Ref. 15
L	$2.90 \times 10^9 - 1.17 \times 10^7\ T$, $\frac{\text{dyne-cm.}}{\text{gm}}$	Straight line fit to data from Ref. 15

Vapor pressure —

above the triple point

$$\frac{1}{T} = 1.666 \times 10^{-2} - 3.218 \times 10^{-3} \log p - 1.015 \times 10^{-5} \log^2 p$$

below the triple point

$$\frac{1}{T} = 1.655 \times 10^{-2} - 2.787 \times 10^{-3} \log p$$

} Least squares fits to data from Ref. 16

TABLE II

INPUT DATA FOR CONDENSATION CALCULATIONS

Calculation	A* (cm^2)	θ (deg.)	$\bar{r}$ (cm)	p_o (psia)	T_o (^oK)	Remarks
Nagamatsu-Willmarth	0.06452	9.75	($\bar{h}$ = .36)	122.3	298	Wedge nozzle, 1.0 cm. wide These inputs are used as the basis for the heterogeneous condensation calculations
Daum:						
M = 10 Nozzle	0.08511	7.31	1.28	228	varied	M = 9.4 at nozzle exit, x_{exit} = 9.60 in.
M = 15 Nozzle	0.01216	5.99	0.59	700	varied	M = 13 at nozzle exit,
M = 15 Nozzle	0.01216	5.99	0.59	574	varied	x_{exit} = 9.88 in.
Parametric Study:						
Variation of geometrical expansion rate	0.0507	5.00	1.46	100, 1000, 5000	298	
	0.0507	10.00	0.72			
	0.0507	15.00	0.47			
	0.0507	20.00	0.35			
	0.0507	30.00	0.22			
	0.0127	5.06	0.72			
	0.203	19.42	0.72			
	0.203	10.00	1.44			
	1.268	10.00	3.60			
p_o variation	0.0507	10.0	0.72	5-7500	298	
T_o variation	0.0507	10.0	0.72	1000	298, 450, 700, 1100	

TABLE II (cont.)

INPUT DATA FOR CONDENSATION CALCULATIONS

Calculation	A* (cm^2)	θ (deg.)	$\bar{r}$ (cm)	p_o (psia)	T_o (^oK)	Remarks
Constant entropy	0.0507	10.0	0.72	2.79×10^{-1}	55.5	
	↓	↓	↓	3.66×10^{-1}	60.0	
				2.19×10^{0}	100.0	All p_o, T_o combinations
				1.00×10^{2}	298.0	lie on the isentrope defined
				6.91×10^{3}	1000.0	
				7.83×10^{4}	2000.0	by p_o = 100 psia, T_o = 298^{o}K.

TABLE III

RESULTS OF THE PARAMETRIC STUDY OF CONDENSATION ONSET IN MOLECULAR NITROGEN

Parameter	Δx_i	T_{sat}	M_{sat}	p_c	T_c	$T_{i,c}$	u_c	$M_{i,c}$	$\Delta T_{i,c}$	$\left(-\frac{1}{\rho}\frac{d\rho}{dt}\right)_{i,c}$	$Z_{i,c}$
	(10^{-3} cm)	(^oK)		(psia)	(^oK)	(^oK)	($10^5 \frac{cm}{sec}$)		(^oK)	(10^4 sec^{-1})	($x10^{11}$)
Variation of Geometrical Expansion Rate											
$\bar{r}$(cm) θ (deg)											
p_0 = 100 psia:											
1.46 5.00	10.0	55.16	4.69	5.92×10^{-2}	35.88	35.49	0.74	6.08	19.67	1.39	.634
0.72 10.00	5.0	55.16	4.69	5.36×10^{-2}	34.89	34.60	0.74	6.17	20.46	2.73	1.24
0.47 15.00	3.5	55.16	4.69	5.06×10^{-2}	34.31	34.00	0.74	6.23	21.16	4.05	1.85
0.35 20.00	2.5	55.16	4.69	4.84×10^{-2}	33.88	33.53	0.74	6.28	21.63	5.42	2.47
0.22 30.00	2.0	55.16	4.69	4.56×10^{-2}	33.27	32.96	0.74	6.34	22.20	8.43	3.85
0.72 5.06	5.0	55.16	4.69	5.36×10^{-2}	34.89	34.60	0.74	6.17	20.56	2.73	1.24
0.72 19.42	5.0	55.16	4.69	5.36×10^{-2}	34.89	34.60	0.74	6.17	20.56	2.73	1.24
1.44 10.00	10.0	55.16	4.69	5.92×10^{-2}	35.87	35.49	0.74	6.08	19.67	1.40	.642
3.60 10.00	25.0	55.16	4.69	6.67×10^{-2}	37.15	36.77	0.74	5.96	18.39	.586	.267
p_0 = 1000 psia:											
1.46 5.00	2.00	71.46	3.98	2.57	54.72	54.06	0.71	4.75	17.40	2.26	.103
0.72 10.00	1.25	71.46	3.98	2.43	53.85	53.13	0.71	4.80	18.33	4.49	.205
0.47 15.00	1.00	71.46	3.98	2.35	53.29	52.60	0.71	4.83	18.86	6.68	.305
0.35 20.00	0.80	71.46	3.98	2.28	52.87	52.24	0.71	4.85	19.22	9.08	.414
0.22 30.00	0.50	71.46	3.98	2.19	52.23	51.52	0.71	4.89	19.94	14.1	.646
0.72 5.06	1.25	71.46	3.98	2.43	53.85	53.13	0.71	4.80	18.33	4.49	.205
0.72 19.42	1.25	71.46	3.98	2.43	53.85	53.13	0.71	4.80	18.33	4.49	.205
1.44 10.00	2.00	71.46	3.98	2.57	54.72	54.06	0.71	4.75	17.40	2.26	.103
3.60 10.00	4.00	71.46	3.98	2.74	55.72	55.01	0.71	4.70	16.45	.931	.0425

TABLE III (cont)

RESULTS OF THE PARAMETRIC STUDY OF CONDENSATION ONSET IN MOLECULAR NITROGEN

Parameter	Δx_i	T_{sat}	M_{sat}	p_c	T_c	$T_{i,c}$	u_c	$M_{i,c}$	$\Delta T_{i,c}$	$\left(-\frac{1}{\rho}\frac{d\rho}{dt}\right)_{i,c}$	$Z_{i,c}$
	(10^{-3} cm)	(^oK)		(psia)	(^oK)	(^oK)	($10^5 \frac{cm}{sec}$)		(^oK)	(10^4 sec^{-1})	($x10^{11}$)
Variation of Geometrical Expansion Rate (cont)											
$\bar{r}$(cm) θ(deg)											
p_0 = 5000 psia:											
0.22 30.0	0.20	98.72	3.18	6.07 x 10	85.59	84.30	0.66	3.56	14.42	24.6	.225
0.35 20.0	0.25	98.72	3.18	6.21 x 10	86.13	84.99	0.66	3.54	13.73	15.5	.142
0.47 15.0	0.35	98.72	3.18	6.31 x 10	86.54	85.35	0.66	3.53	13.37	11.6	.106
0.72 10.0	0.50	98.72	3.18	6.44 x 10	86.97	85.68	0.66	3.52	13.04	7.52	.0687
1.46 5.0	0.75	98.72	3.18	6.52 x 10	87.72	86.39	0.66	3.50	12.33	3.78	.0347
3.60 10.0	1.50	98.72	3.18	6.83 x 10	88.53	87.08	0.66	3.48	11.64	1.55	.0142
Variation of p_0											
p_0 (psia)											
5	20.00	44.04	5.37	3.83×10^{-4}	19.88	19.81	0.76	8.38	24.23	1.40	12.7
10	20.00	46.14	5.22	1.28×10^{-3}	23.05	22.90	0.76	7.75	23.24	1.82	8.31
20	10.00	48.49	5.07	3.83×10^{-3}	25.93	25.76	0.75	7.27	22.73	1.92	4.39
50	7.50	52.05	4.86	1.73×10^{-2}	30.75	30.52	0.75	6.62	21.53	2.35	2.15
100	5.00	55.16	4.69	5.36×10^{-2}	34.89	34.60	0.74	6.17	20.46	2.73	1.24
200	3.50	58.74	4.51	1.67×10^{-1}	39.62	39.28	0.73	5.74	19.46	3.17	.775
300	3.40	61.10	4.40	3.25×10^{-1}	42.70	42.26	0.73	5.50	18.84	3.45	.525
500	2.00	64.71	4.25	7.57×10^{-1}	47.00	46.52	0.72	5.20	18.19	3.85	.351
700	2.10	67.78	4.12	1.33	50.11	49.50	0.72	5.01	18.28	4.13	.270
900	1.80	70.32	4.02	2.03	52.67	52.06	0.71	4.86	18.26	4.39	.220
1000	1.25	71.46	3.98	2.43	53.85	53.13	0.71	4.80	18.33	4.49	.205

TABLE III (cont)

RESULTS OF THE PARAMETRIC STUDY OF CONDENSATION ONSET IN MOLECULAR NITROGEN

Parameter	Δx_i	T_{sat}	M_{sat}	p_c	T_c	$T_{i,c}$	u_c	$M_{i,c}$	$\Delta T_{i,c}$	$\left(-\frac{1}{\rho}\frac{d\rho}{dt}\right)_{i,c}$	$Z_{i,c}$
	(10^{-3} cm)	(^oK)		(psia)	(^oK)	(^oK)	($10^5 \frac{cm}{sec}$)		(^oK)	(10^4 sec^{-1})	($x10^{11}$)
Variation of p_0 (cont)											
p_0 (psia)											
1500	1.30	76.34	3.81	4.91	58.68	57.96	0.71	4.55	18.38	4.95	.151
2000	1.20	80.40	3.68	8.20	62.58	61.84	0.70	4.37	18.56	5.33	.122
2500	0.90	83.97	3.57	1.31 x 10	67.09	66.31	0.69	4.18	17.66	5.78	.105
3000	0.80	87.23	3.48	1.94 x 10	71.33	70.42	0.69	4.02	16.81	6.18	.0940
4000	0.60	93.19	3.32	3.74 x 10	79.29	78.17	0.68	3.75	15.02	6.90	.0788
5000	0.50	98.72	3.18	6.44 x 10	86.97	85.68	0.66	3.52	13.04	7.52	.0687
7500	0.20	112.00	2.88	1.95×10^2	107.24	105.07	0.63	3.03	6.93	9.43	.0574
Variation of T_0											
T_0 (^oK)											
298	1.25	71.46	3.98	2.43	53.85	53.13	0.71	4.80	18.33	4.49	.205
450	6.00	59.69	5.72	2.27×10^{-1}	41.26	40.82	0.92	7.08	18.87	2.50	.483
700	20.00	52.07	7.89	1.91×10^{-2}	31.61	31.33	1.18	10.33	20.74	1.32	1.20
1100	75.00	46.25	10.67	1.56×10^{-3}	24.23	24.10	1.49	14.94	22.15	.689	3.05
Constant Initial Entropy											
T_0 (^oK)											
55.5	0.60	55.16	0.18	4.80×10^{-2}	33.74	33.59	0.21	1.81	21.57	7.08	3.23
60.0	0.75	55.16	0.66	4.79×10^{-2}	33.73	33.48	0.23	1.99	21.68	6.73	3.07
100.0	1.80	55.16	2.02	4.85×10^{-2}	34.04	33.79	0.37	3.13	21.37	5.23	2.39
298.0	5.00	55.16	4.69	5.36×10^{-2}	34.89	34.60	0.74	6.17	20.46	2.73	1.24
1000.0	20.00	55.16	9.26	6.03×10^{-2}	36.11	35.77	1.41	11.61	19.39	1.20	.545
2000.0	50.00	55.16	13.28	6.46×10^{-2}	36.82	36.46	2.02	16.41	18.70	.738	.337

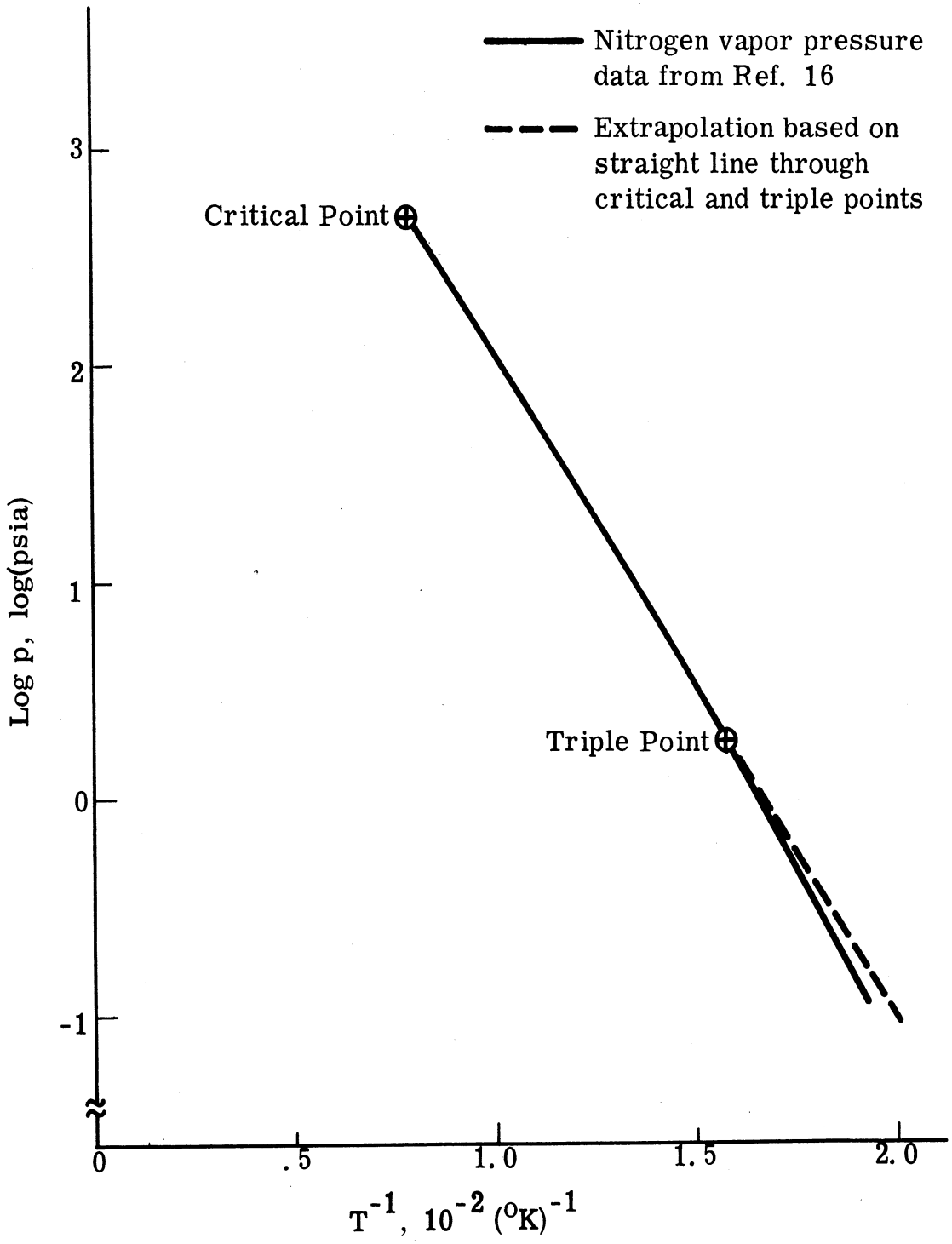

Figure 1. Nitrogen Vapor Pressure Curve

Figure 2. Effect of Tolman Constant, D, on Computed Condensation History: Pressure vs. Temperature.

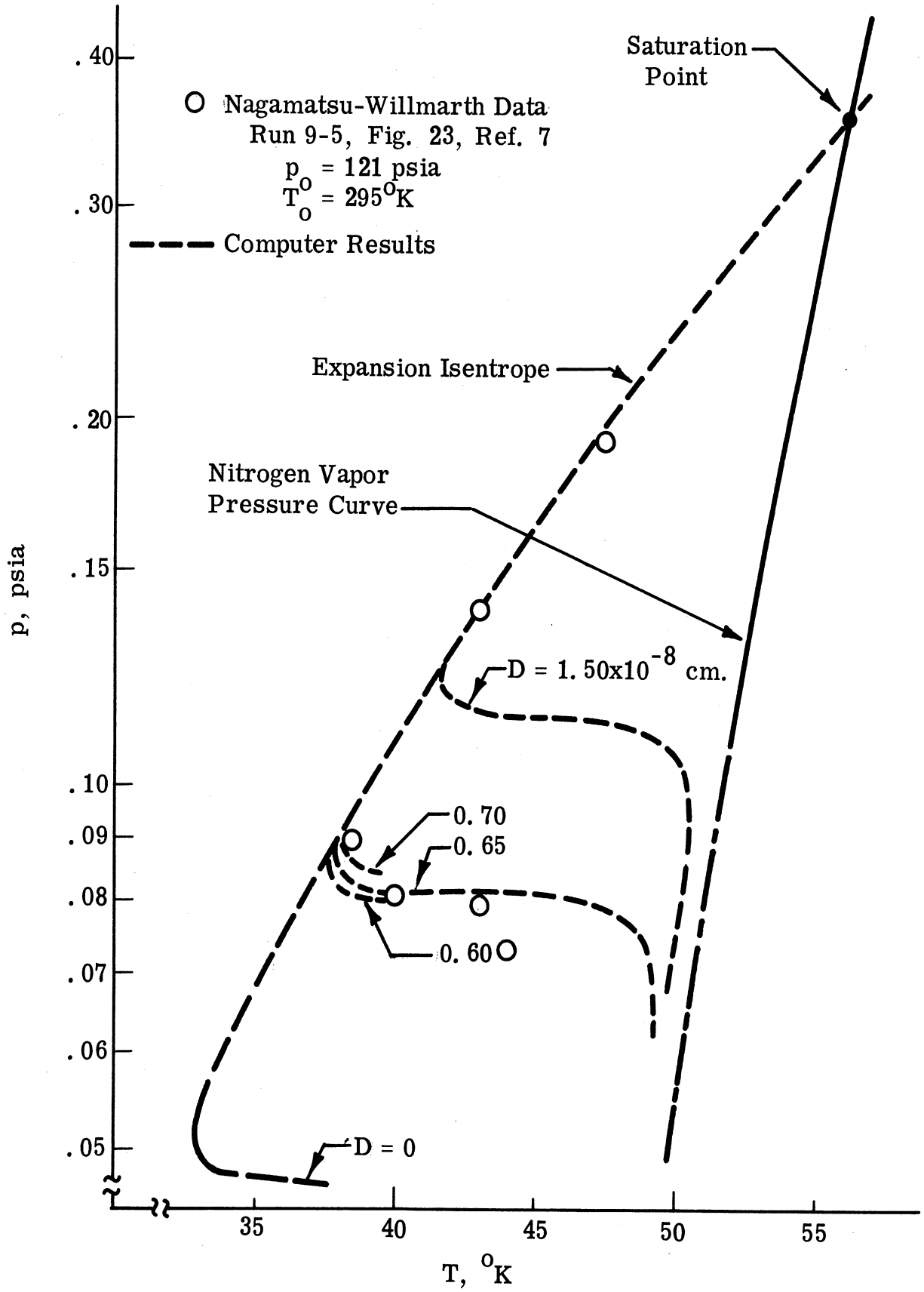

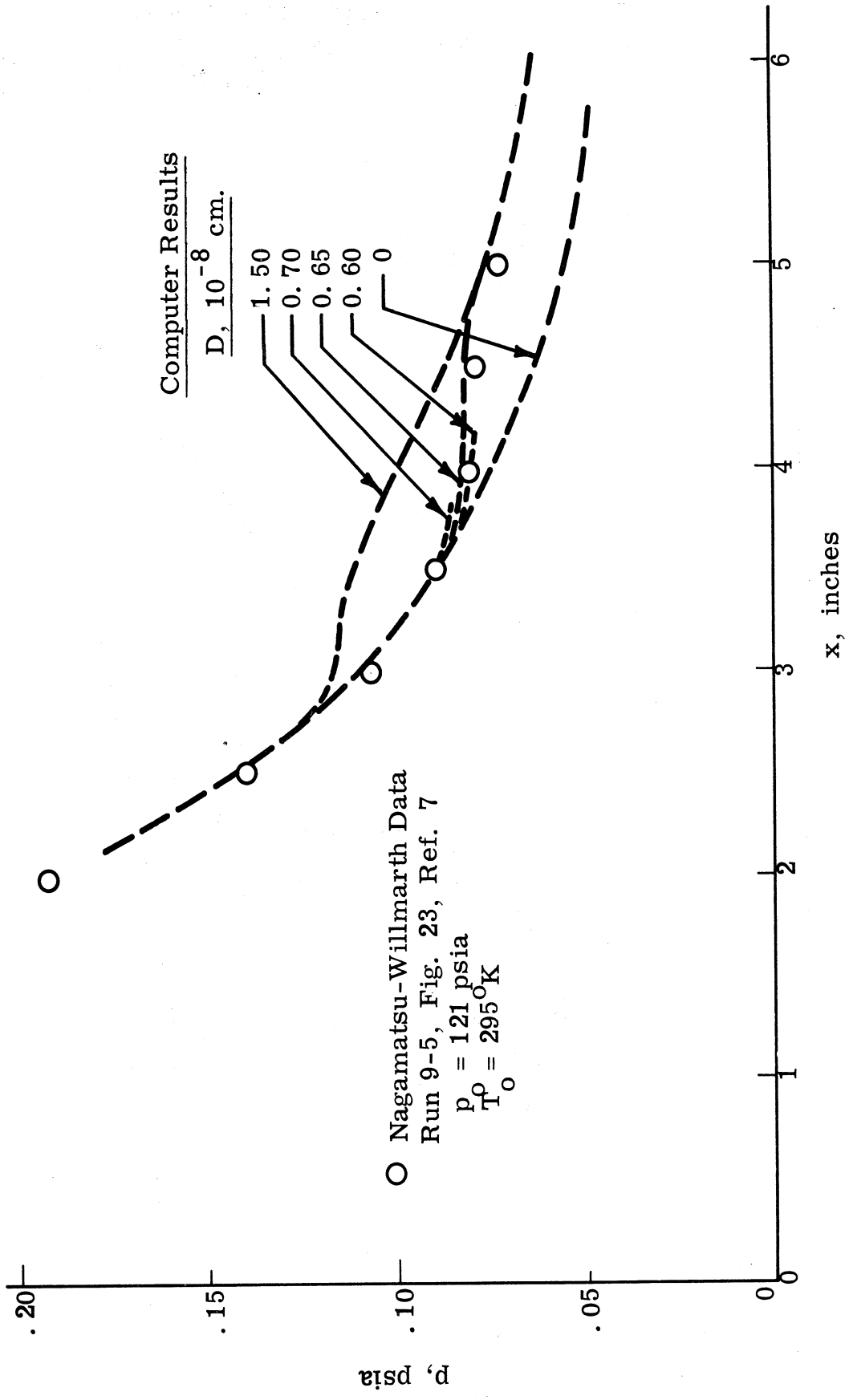

Figure 3. Effect of Tolman Constant, D, on Computed Condensation History: Pressure vs. Distance.

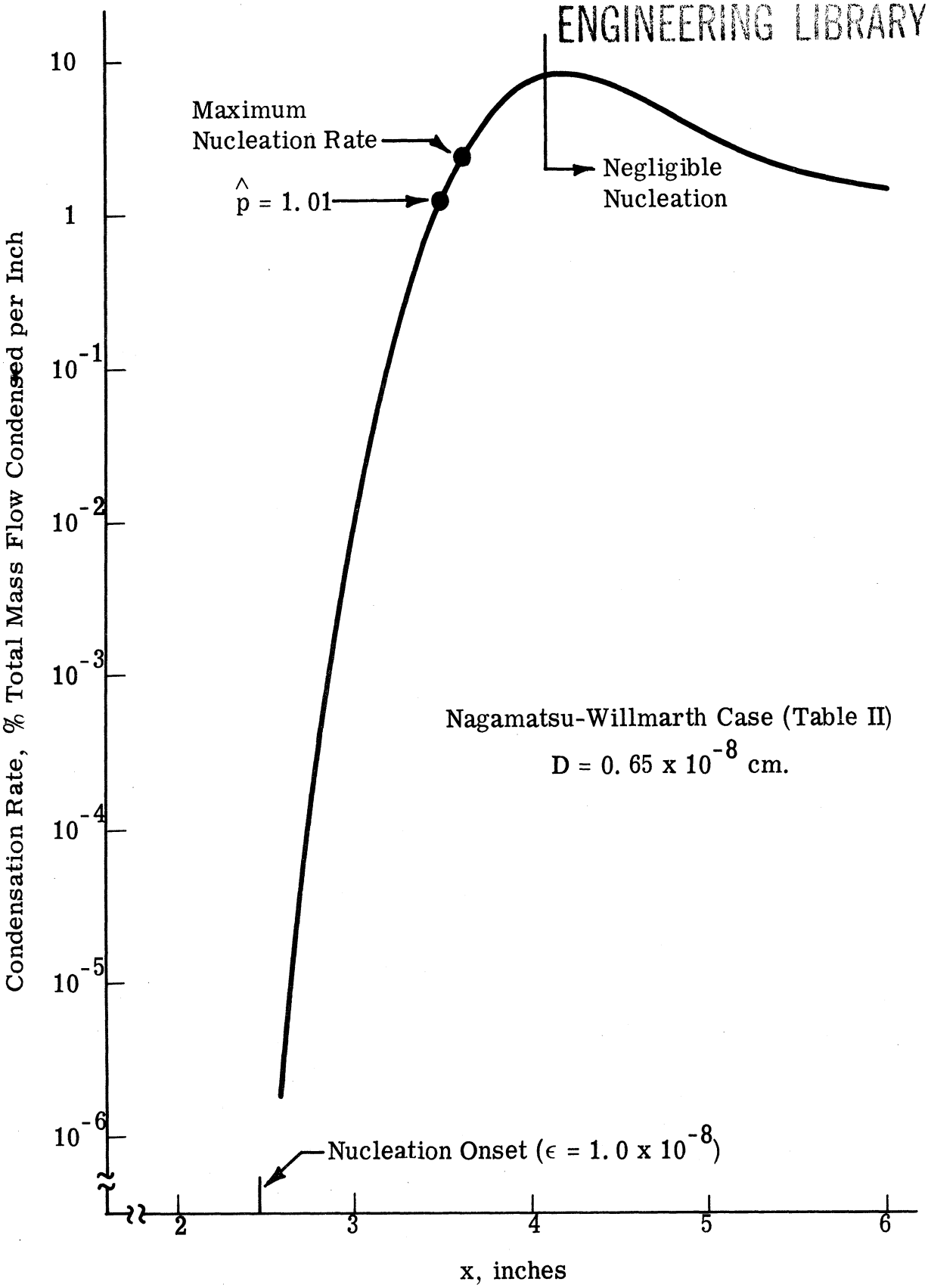

Figure 4. Calculated Condensation Rate History in Nitrogen

Figure 5. Heterogeneous Condensation: Effect of Foreign Nuclei on Condensation History.

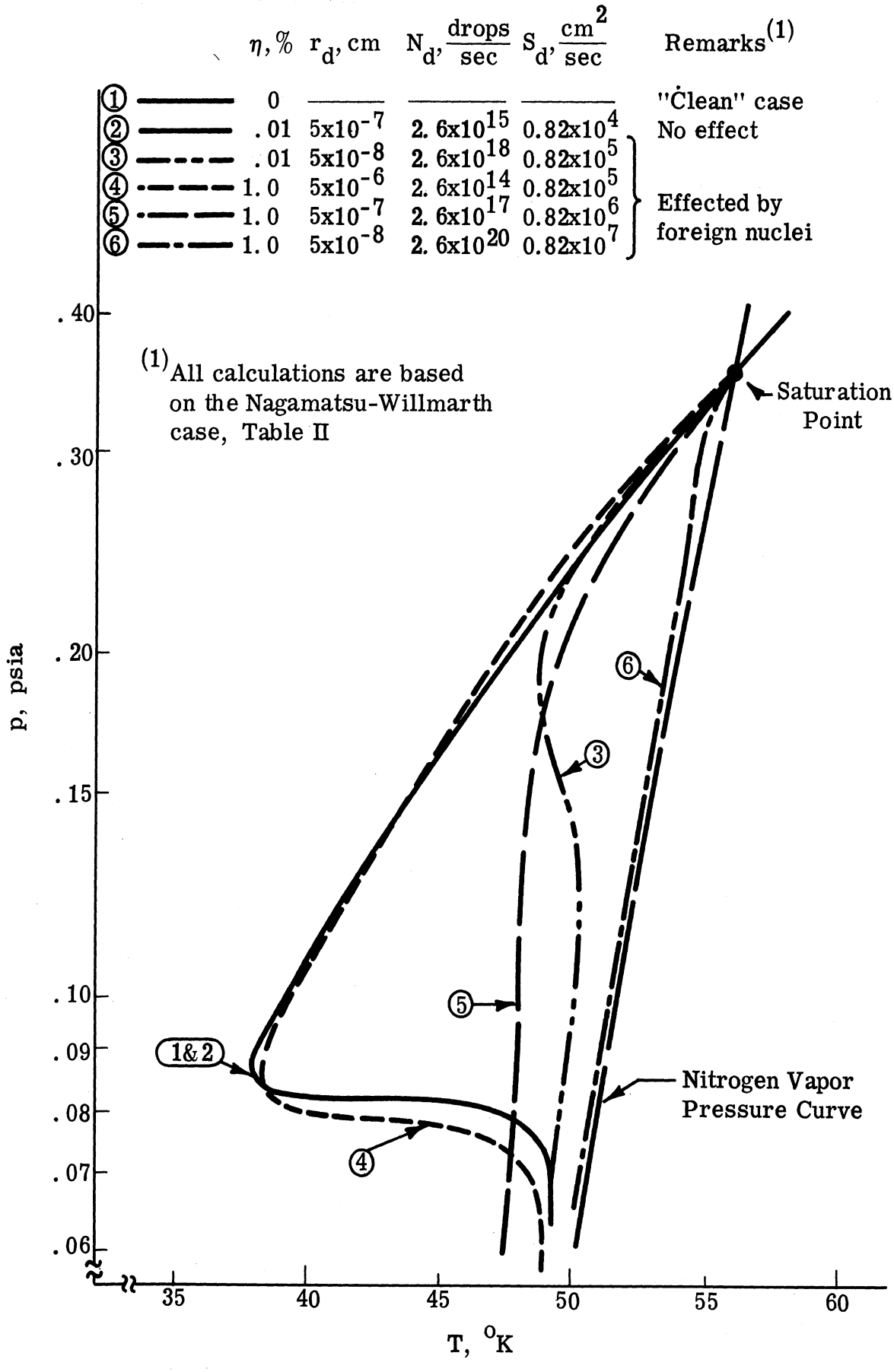

Figure 6. Effect of ϵ and initial Δx on Calculated Condensation Temperature.

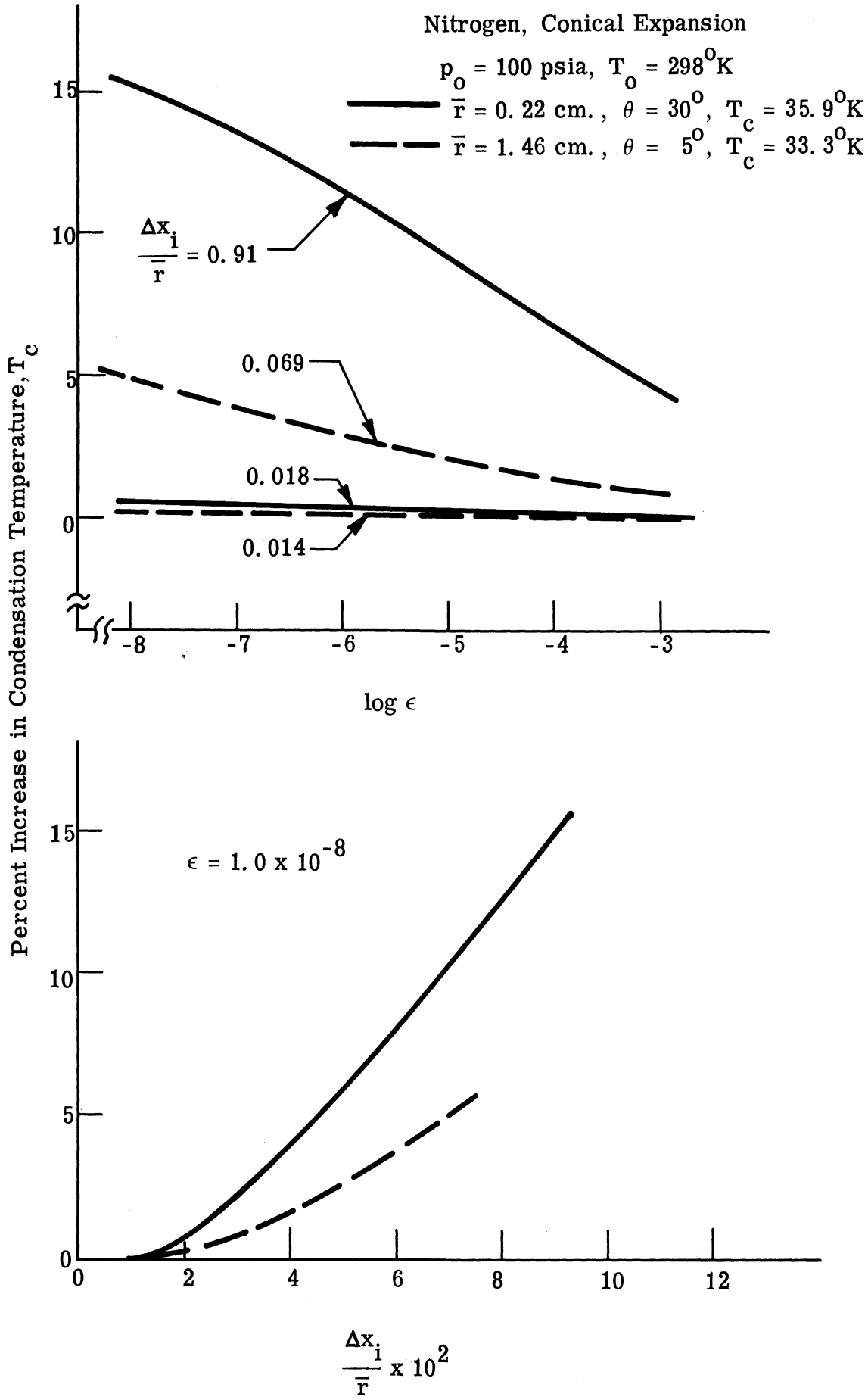

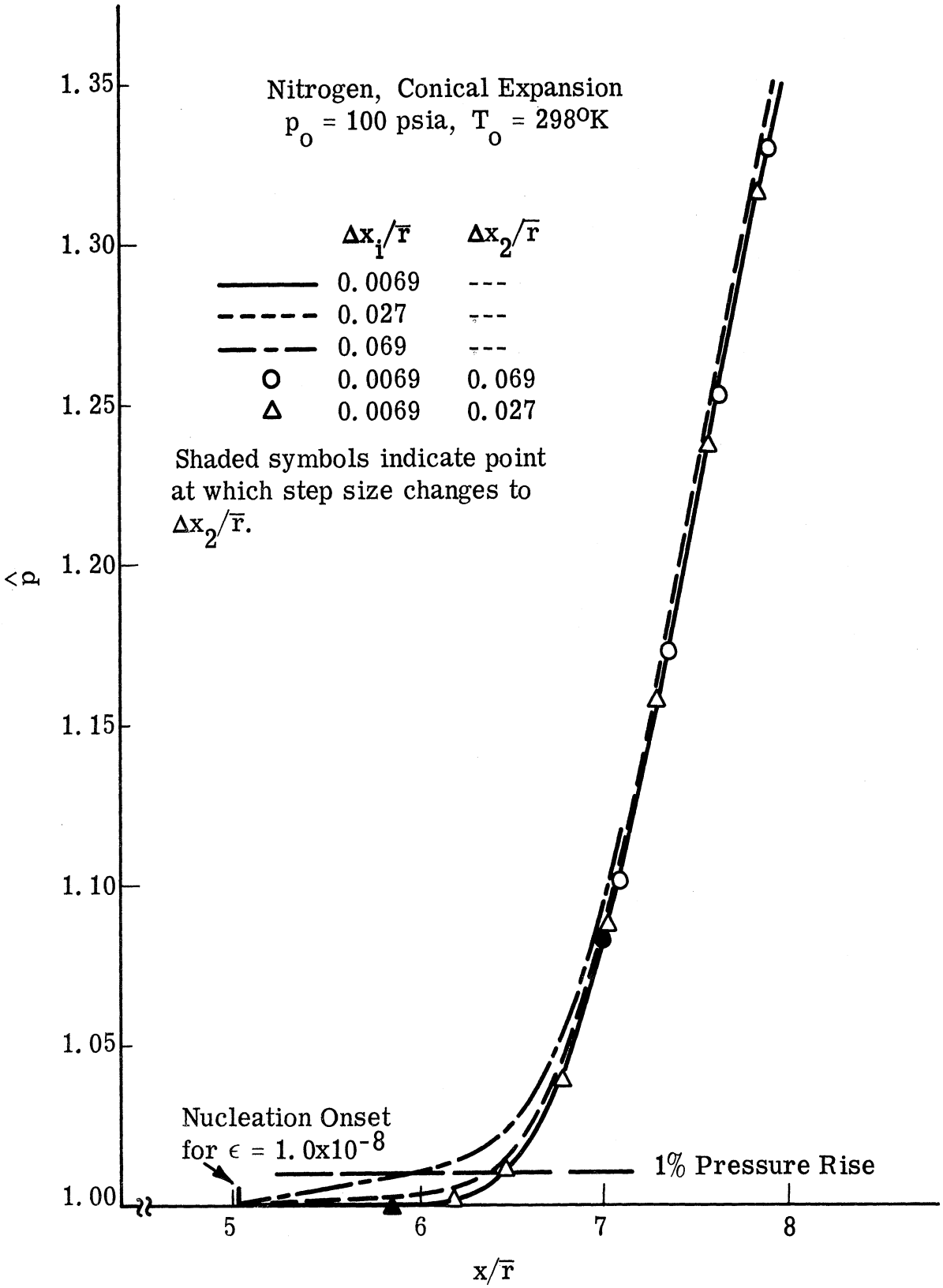

Figure 7. Effect of Δx on Pressure vs. Distance Condensation History.

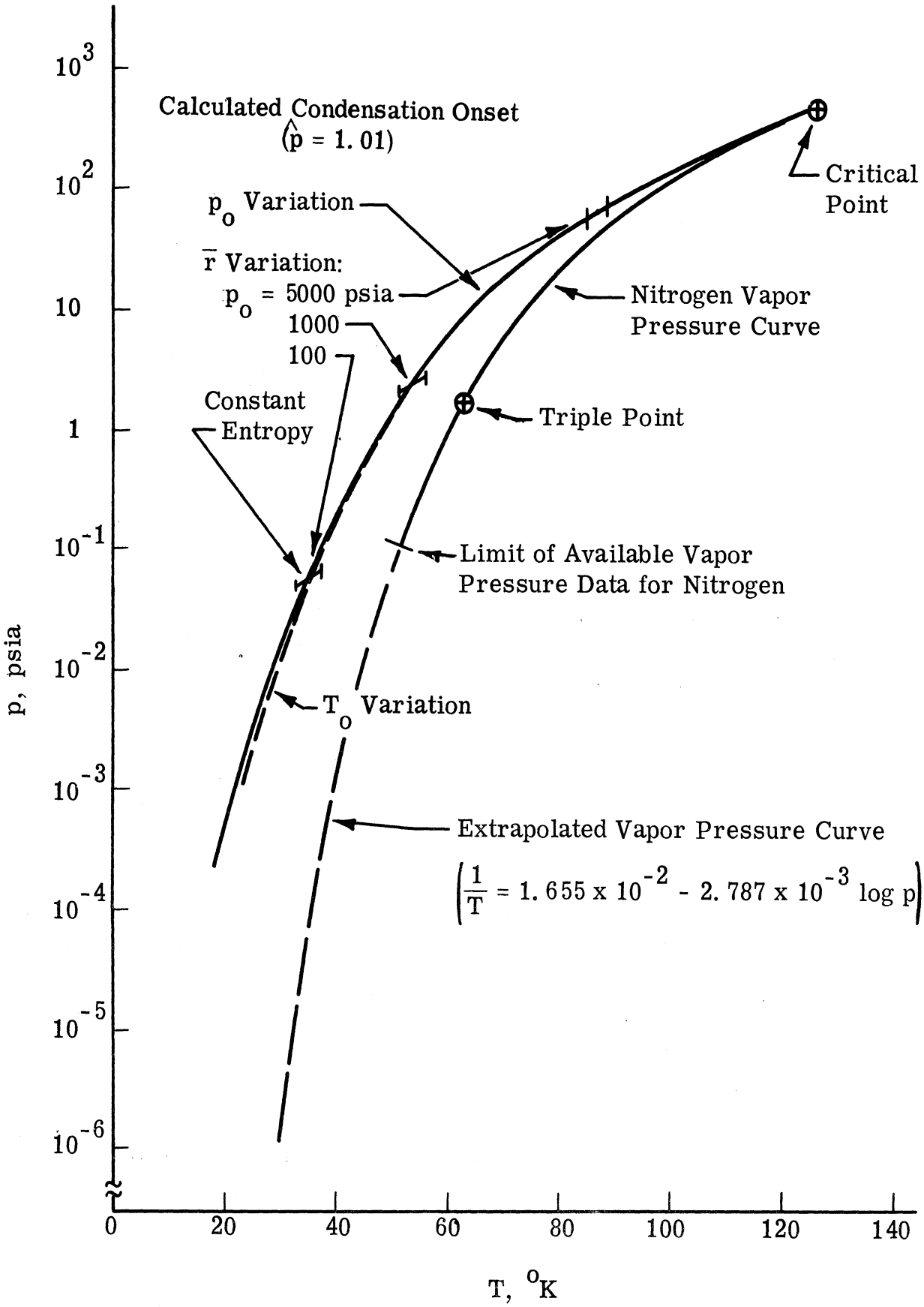

Figure 8. Summary of Results from Parametric Study of Condensation Onset.

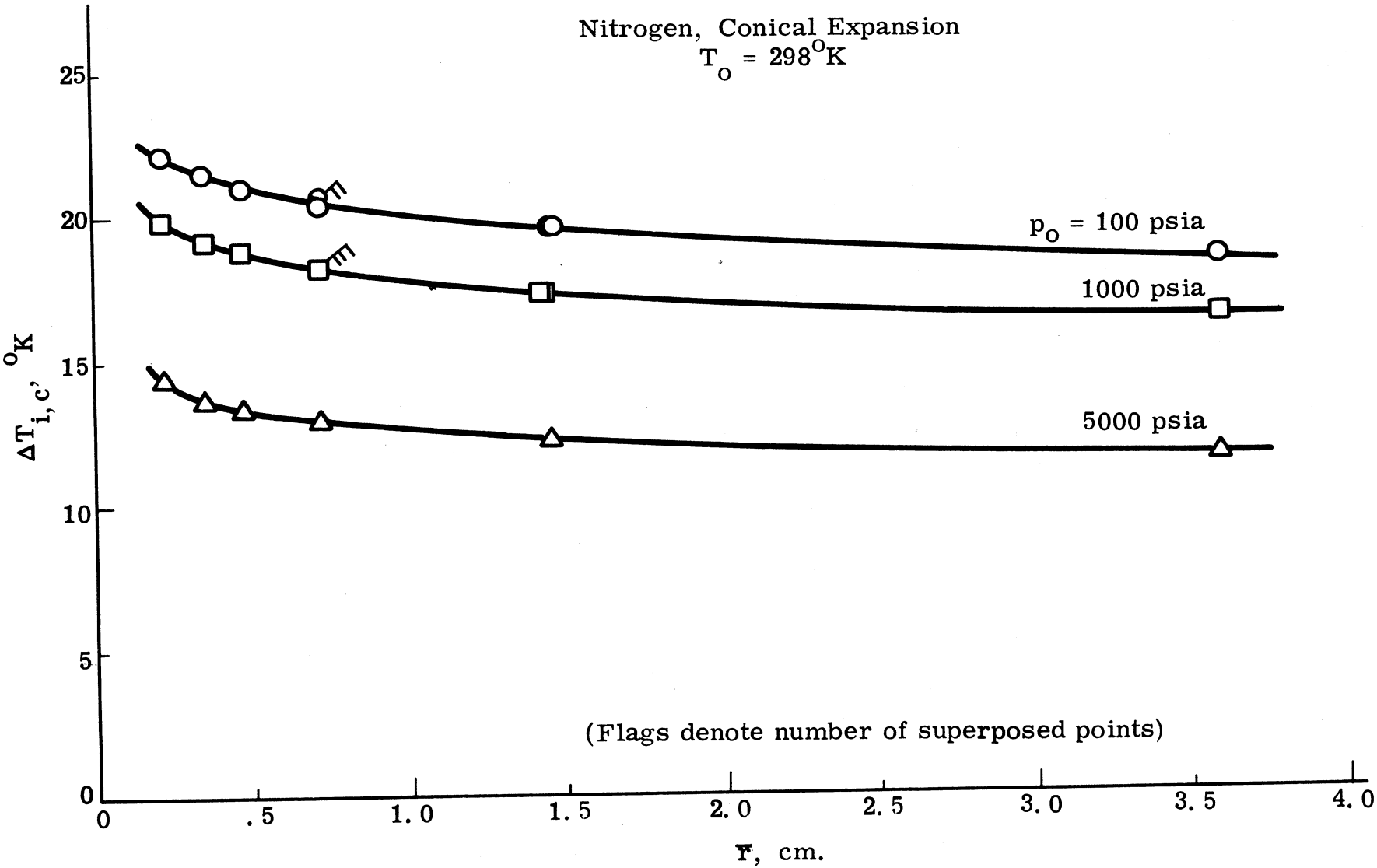

Figure 9. Effect of Geometrical Expansion Rate on Calculated Supersaturation Temperature Decrement, $\Delta T_{i,c'}$.

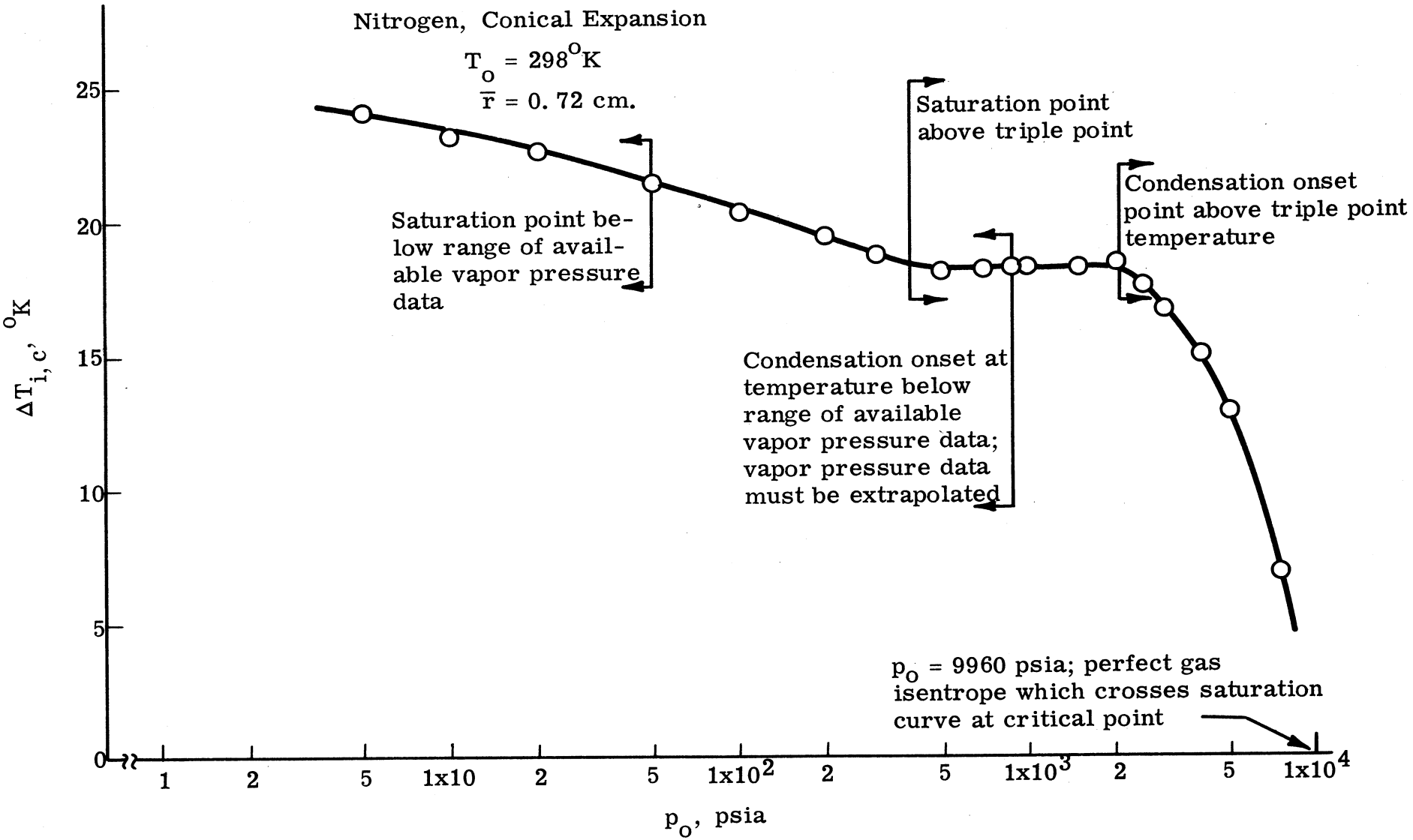

Figure 10. Effect of Initial Pressure on Calculated Supersaturation Temperature Decrement, $\Delta T_{i,c}$.

Figure 11. Effect of Initial Temperature on Calculated Supersaturation Temperature Decrement, $\Delta T_{i,c}$.

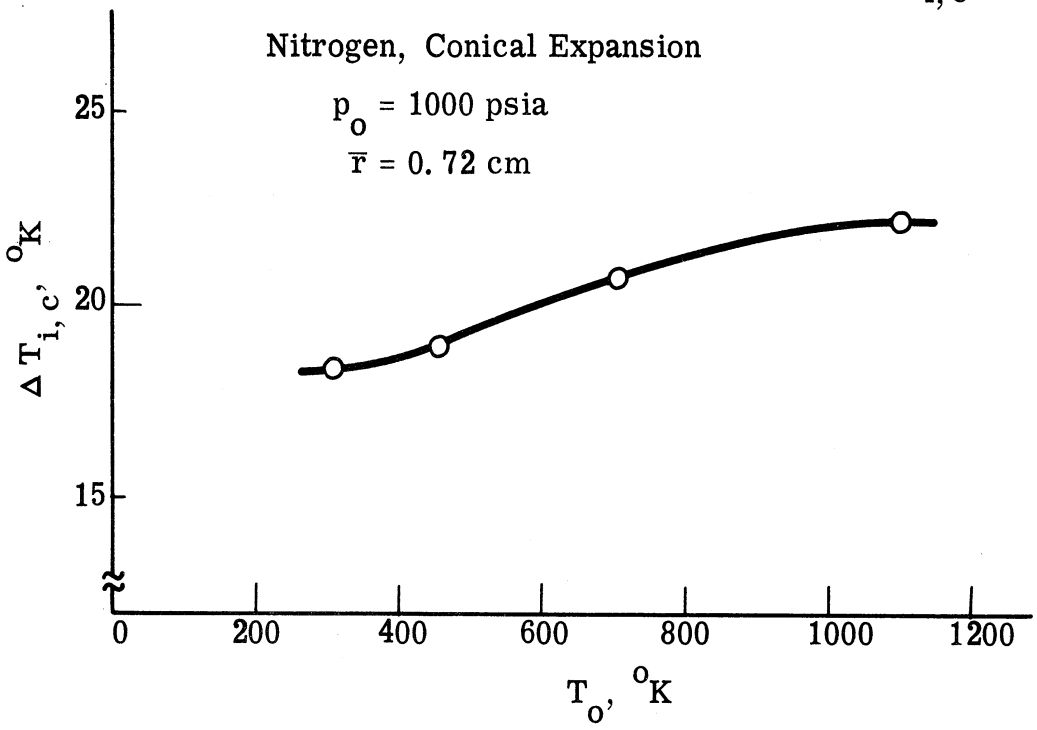

Figure 12. Effect of Initial Temperature (for Fixed Initial Entropy) on Calculated Supersaturation Temperature Decrement, $\Delta T_{i,c}$.

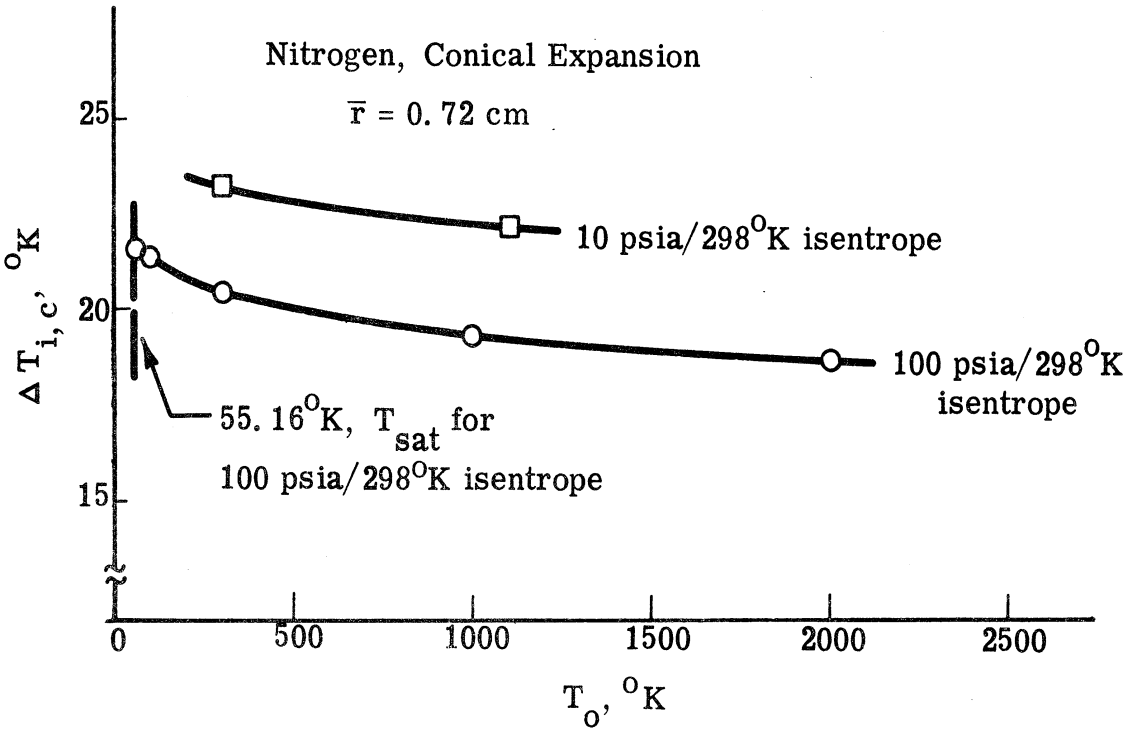

Figure 13. Correlation of Calculated Condensation Onset Results with Rate of Change of Vapor Density.

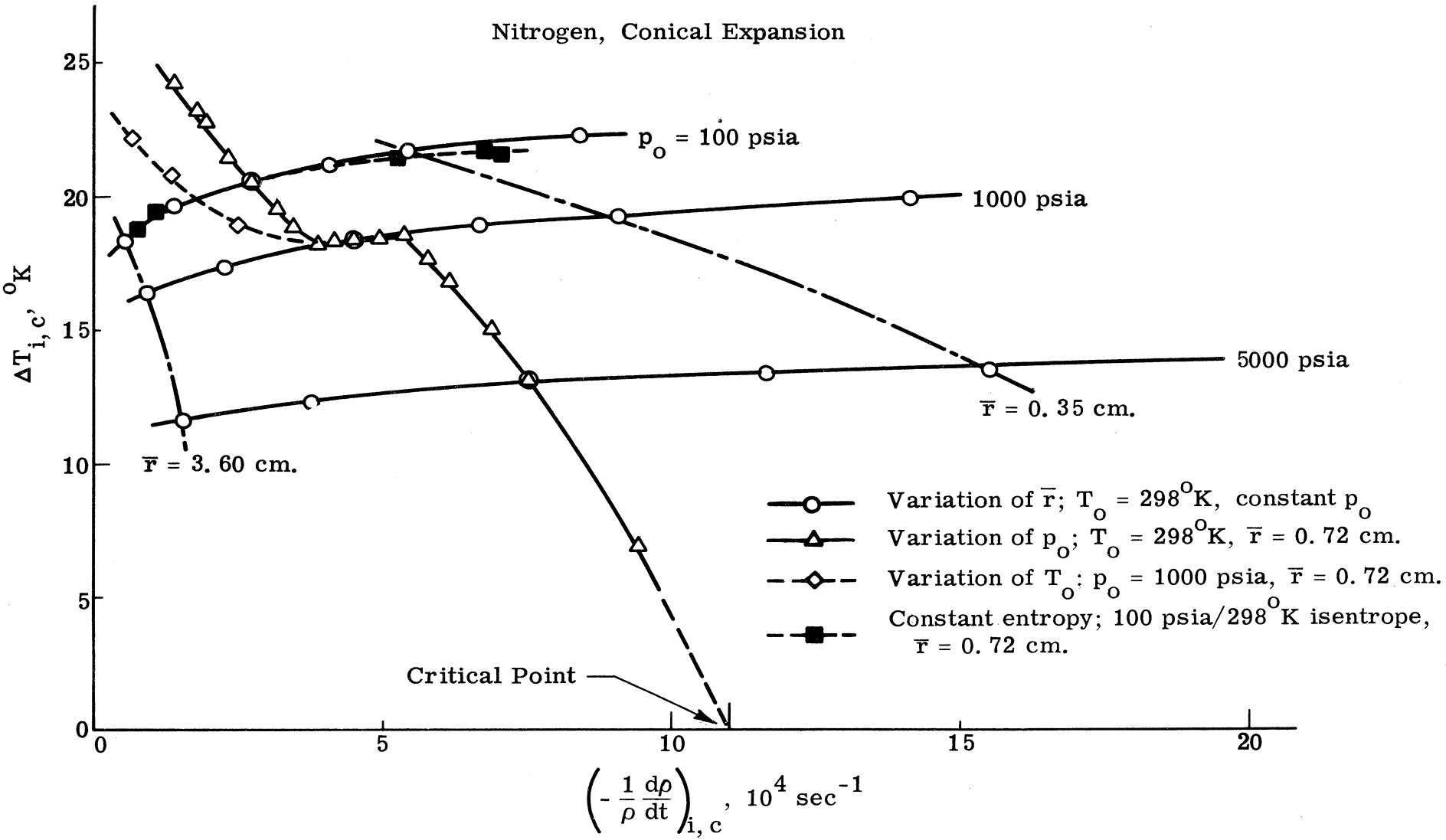

Figure 14. Correlation of Calculated Condensation Onset Results with Parameter $Z_{i,c}$.

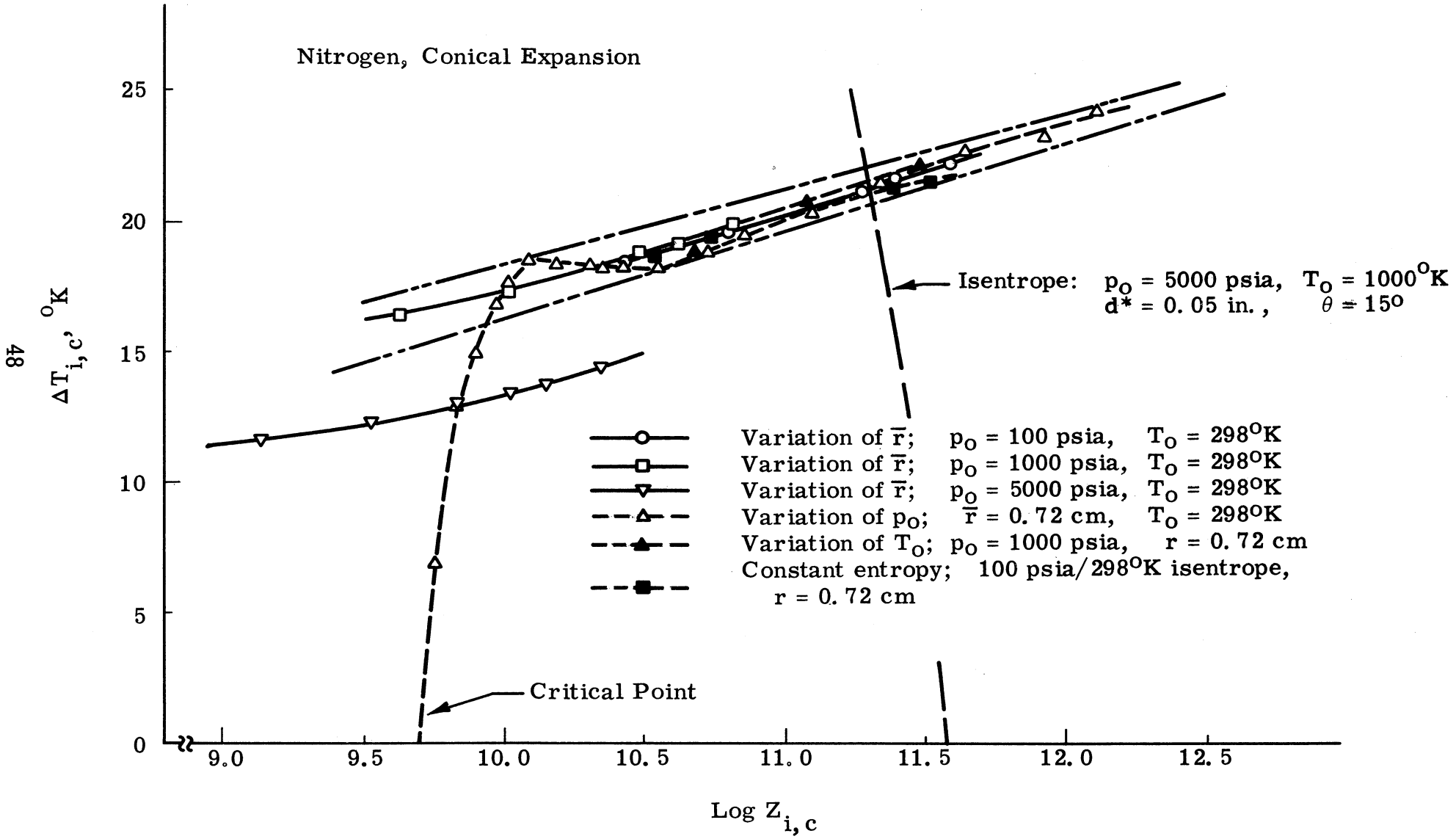

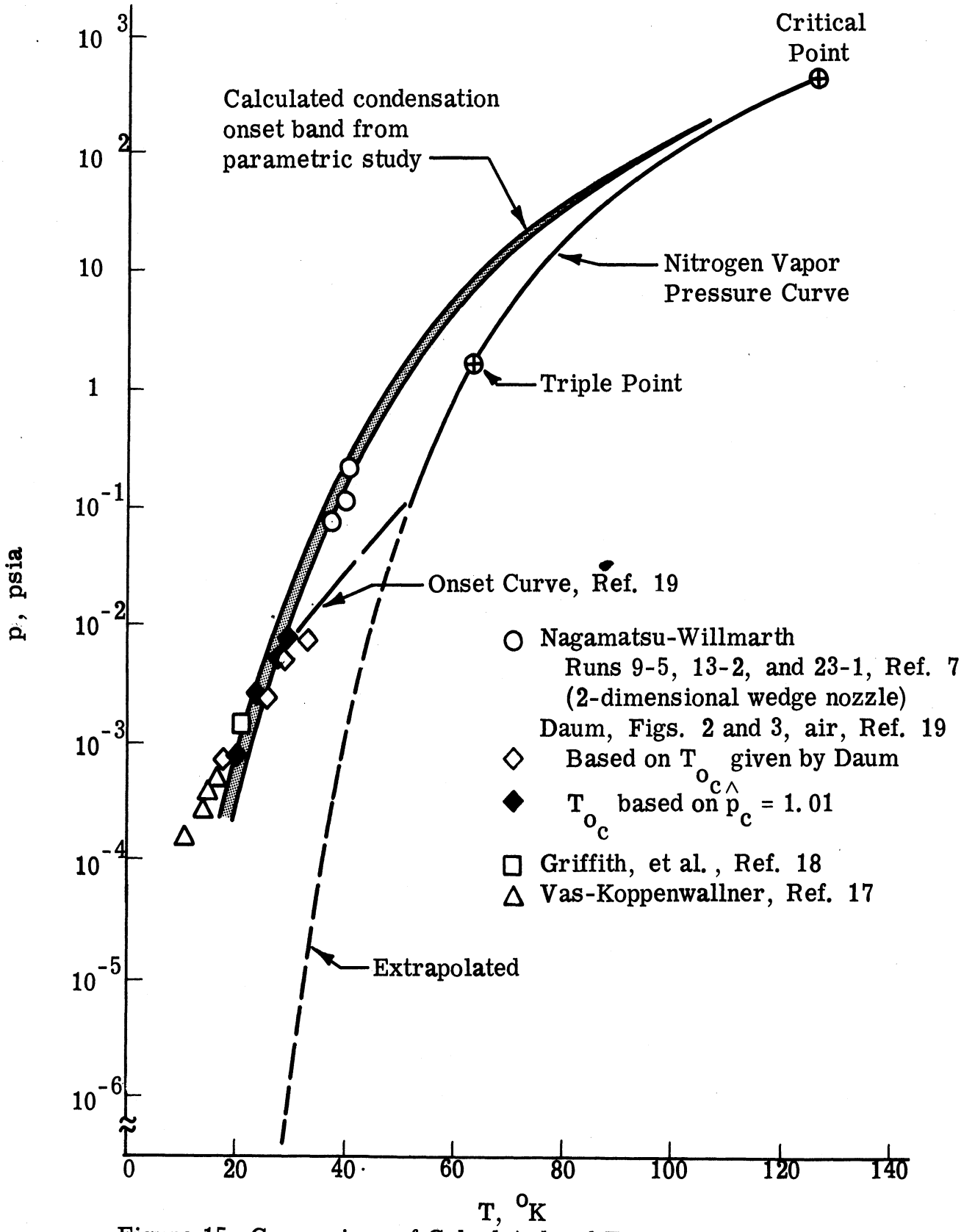

Figure 15. Comparison of Calculated and Experimental Condensation Onset Results: Pressure vs. Temperature.

Figure 16. Comparison of Calculated and Experimental Condensation Onset Results Using the Correlation Parameter $Z_{i,c}$.

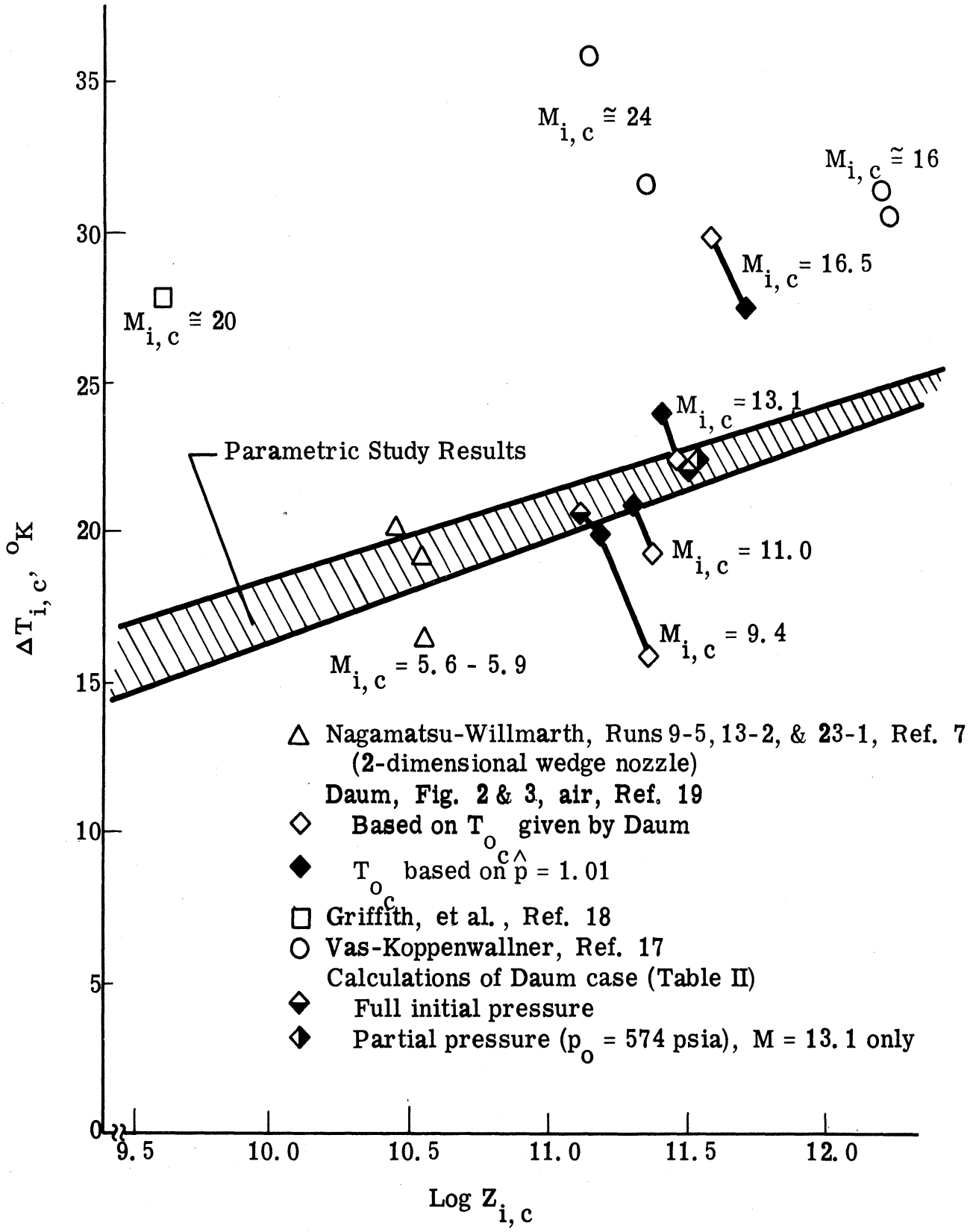

Figure 17. Comparison of the Calculated and Experimental Condensation Produced Pressure Rises at the Exit of the Daum M = 15 Nozzle.

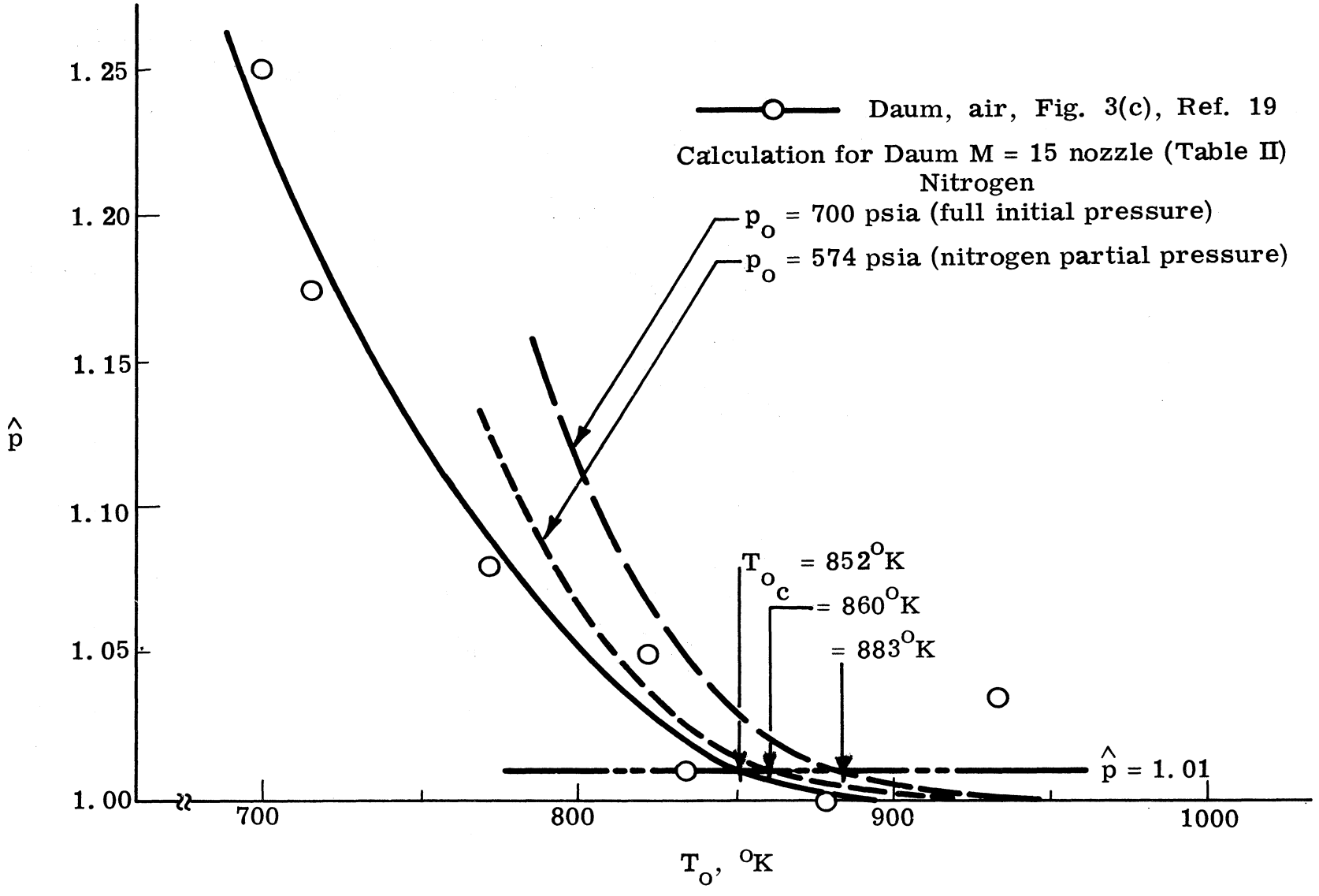

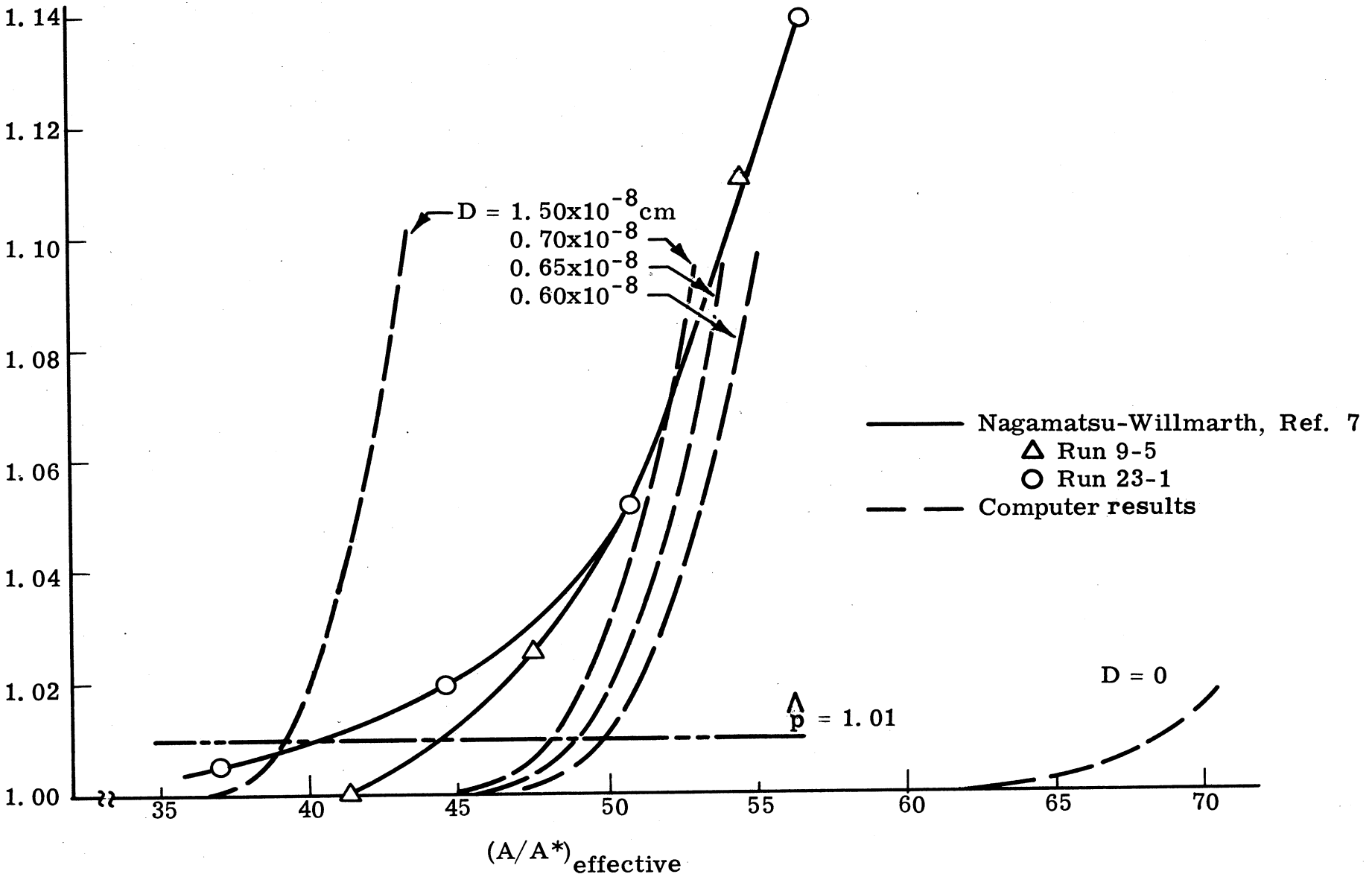

Figure 18. Comparison of the Calculated and Experimental Condensation Produced Pressure Rises in the Nagamatsu-Willmarth Nozzle.

Figure 19. Comparison of Calculated and Experimental Condensation Onset Results: $\text{Log}(p_{i,c}/p_{\infty,c})$ vs. $T_{i,c}^{-3/2}$.

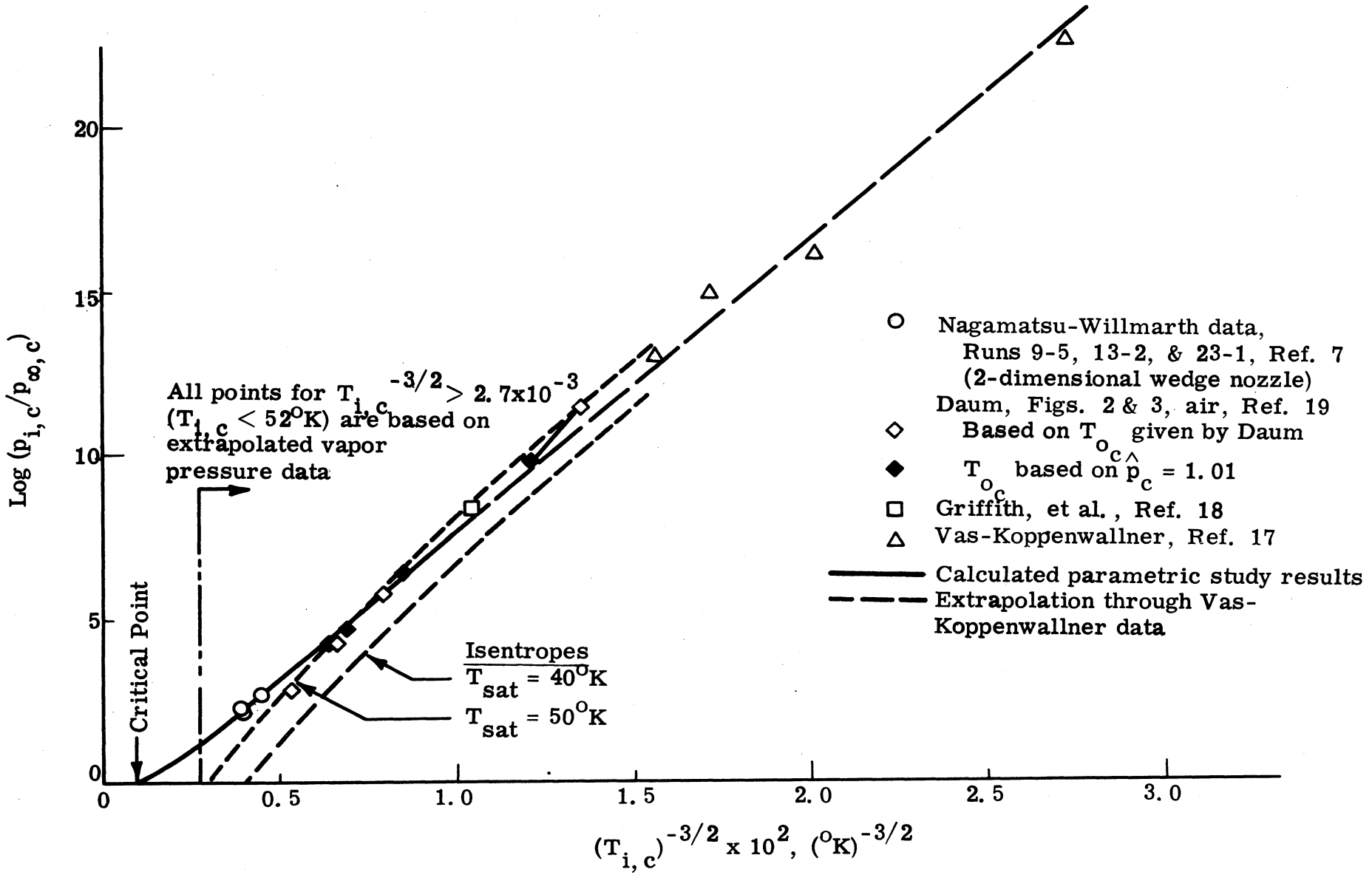

Unclassified
Security Classification

DOCUMENT CONTROL DATA - R&D

(Security classification of title, body of abstract and indexing annotation must be entered when the overall report is classified)

1. ORIGINATING ACTIVITY *(Corporate author)*
University of Michigan
Ann Arbor, Michigan

2a. REPORT SECURITY CLASSIFICATION
Unclassified

2b. GROUP

3. REPORT TITLE
Digital Computer Studies of Condensation in Expanding One-Component Flows

4. DESCRIPTIVE NOTES *(Type of report and inclusive dates)*
Scientific Research Report - Interim TDR

5. AUTHOR(S) *(Last name, first name, initial)*
Sivier, Kenneth R.

6. REPORT DATE	7a. TOTAL NO. OF PAGES	7b. NO. OF REFS
November 1965	53	19

8a. CONTRACT OR GRANT NO.
AF 33(615)-2307
b. PROJECT NO. 7116-01
c. 61445014
d. 681308

9a. ORIGINATOR'S REPORT NUMBER(S)

9b. OTHER REPORT NO(S) *(Any other numbers that may be assigned this report)*
ARL 65-234

10. AVAILABILITY/LIMITATION NOTICES
Distribution of this document is unlimited.

11. SUPPLEMENTARY NOTES

12. SPONSORING MILITARY ACTIVITY
Aerospace Research Laboratories (ARN)
Office of Aerospace Research, USAF
Wright-Patterson AFB, Ohio

13. ABSTRACT

This report discusses a digital computer program for calculating the vapor condensation that occurs in expanding, one-component flows. A discussion is presented of modifications made in Griffin's original program. Emphasis is placed on the reasons for the modifications and their effect on the numerical results.

The results of a parametric study (using the computer program) of condensation onset in nitrogen flows are presented and compared with experimental data. Several methods of presenting and correlating condensation onset data are used. One of these produces a remarkable correlation of the numerical results. The comparison between the experimental and numerical data shows that the computer program is able to reproduce satisfactorily the qualitative features of the condensation produced and to yield a relatively good quantitative picture of condensation onset in nitrogen.

DD FORM 1 JAN 64 1473

Unclassified
Security Classification

Unclassified

Security Classification

14. KEY WORDS	LINK A		LINK B		LINK C	
	ROLE	WT	ROLE	WT	ROLE	WT
Vapor - Condensation Analysis Two-Phase One-Component Flow Analysis Condensation in Expanding Flow						

INSTRUCTIONS

1. ORIGINATING ACTIVITY: Enter the name and address of the contractor, subcontractor, grantee, Department of Defense activity or other organization *(corporate author)* issuing the report.

2*a*. REPORT SECURITY CLASSIFICATION: Enter the overall security classification of the report. Indicate whether "Restricted Data" is included. Marking is to be in accordance with appropriate security regulations.

2*b*. GROUP: Automatic downgrading is specified in DoD Directive 5200.10 and Armed Forces Industrial Manual. Enter the group number. Also, when applicable, show that optional markings have been used for Group 3 and Group 4 as authorized.

3. REPORT TITLE: Enter the complete report title in all capital letters. Titles in all cases should be unclassified. If a meaningful title cannot be selected without classification, show title classification in all capitals in parenthesis immediately following the title.

4. DESCRIPTIVE NOTES: If appropriate, enter the type of report, e.g., interim, progress, summary, annual, or final. Give the inclusive dates when a specific reporting period is covered.

5. AUTHOR(S): Enter the name(s) of author(s) as shown on or in the report. Enter last name, first name, middle initial. If military, show rank and branch of service. The name of the principal author is an absolute minimum requirement.

6. REPORT DATE: Enter the date of the report as day, month, year; or month, year. If more than one date appears on the report, use date of publication.

7*a*. TOTAL NUMBER OF PAGES: The total page count should follow normal pagination procedures, i.e., enter the number of pages containing information.

7*b*. NUMBER OF REFERENCES: Enter the total number of references cited in the report.

8*a*. CONTRACT OR GRANT NUMBER: If appropriate, enter the applicable number of the contract or grant under which the report was written.

8*b*, 8*c*, & 8*d*. PROJECT NUMBER: Enter the appropriate military department identification, such as project number, subproject number, system numbers, task number, etc.

9*a*. ORIGINATOR'S REPORT NUMBER(S): Enter the official report number by which the document will be identified and controlled by the originating activity. This number must be unique to this report.

9*b*. OTHER REPORT NUMBER(S): If the report has been assigned any other report numbers *(either by the originator or by the sponsor)*, also enter this number(s).

10. AVAILABILITY/LIMITATION NOTICES: Enter any limitations on further dissemination of the report, other than those imposed by security classification, using standard statements such as:

(1) "Qualified requesters may obtain copies of this report from DDC."

(2) "Foreign announcement and dissemination of this report by DDC is not authorized."

(3) "U. S. Government agencies may obtain copies of this report directly from DDC. Other qualified DDC users shall request through

_____."

(4) "U. S. military agencies may obtain copies of this report directly from DDC. Other qualified users shall request through

_____."

(5) "All distribution of this report is controlled. Qualified DDC users shall request through

_____."

If the report has been furnished to the Office of Technical Services, Department of Commerce, for sale to the public, indicate this fact and enter the price, if known.

11. SUPPLEMENTARY NOTES: Use for additional explanatory notes.

12. SPONSORING MILITARY ACTIVITY: Enter the name of the departmental project office or laboratory sponsoring *(paying for)* the research and development. Include address.

13. ABSTRACT: Enter an abstract giving a brief and factual summary of the document indicative of the report, even though it may also appear elsewhere in the body of the technical report. If additional space is required, a continuation sheet shall be attached.

It is highly desirable that the abstract of classified reports be unclassified. Each paragraph of the abstract shall end with an indication of the military security classification of the information in the paragraph, represented as *(TS), (S), (C), or (U)*.

There is no limitation on the length of the abstract. However, the suggested length is from 150 to 225 words.

14. KEY WORDS: Key words are technically meaningful terms or short phrases that characterize a report and may be used as index entries for cataloging the report. Key words must be selected so that no security classification is required. Identifiers, such as equipment model designation, trade name, military project code name, geographic location, may be used as key words but will be followed by an indication of technical context. The assignment of links, rules, and weights is optional.

Unclassified

Security Classification